THE INVESTIGATION OF DIVERSE PHYSIOLOGICAL AND THERAPEUTIC IMPACT OF CELLULAR BASED PRODUCTS DERIVED FROM HUMAN CUMULUS CELLS

by
Derya Burukçu

Submitted to Graduate School of Natural and Applied Sciences
in Partial Fulfillment of the Requirements
for the Degree of Master of Science in
Biotechnology

Yeditepe University
2020

THE INVESTIGATION OF DIVERSE PHYSIOLOGICAL AND THERAPEUTIC IMPACT OF CELLULAR BASED PRODUCTS DERIVED FROM HUMAN CUMULUS CELLS

APPROVED BY:

Prof. Dr. Fikrettin Şahin ……
(Thesis Supervisor)
(Yeditepe University)

Prof. Dr. Gamze Torun Köse ……
(Yeditepe University)

Assist. Prof. Dr. Hüseyin Abdik ……
(İstanbul Sabahattin Zaim University)

DATE OF APPROVAL: …./…./2020

ACKNOWLEDGEMENTS

First and foremost, I would like to extend my sincere gratitude to my thesis supervisor Prof. Dr. Fikrettin Şahin, for all the supports he gave me. He has always offered me new opportunities and I am grateful for that. His guidance and encouragement are invaluable to me.

My special words of thanks should also go to Dr. Esra Aydemir. She is not only a tremendous mentor for my thesis but also an inspirer, a role model, and a friend whenever I need her. Besides sharing her endless knowledge and experience with me, she has taught me to look at life from different perspectives. When I lost my motivation and faced with difficulties, she never allowed things to get tedious or dull. Without her guidance, this thesis would not have been achievable.

My acknowledgment would be imperfective without thanking the greatest source of my strength, my family that has always been there for me with their unwavering and unselfish love. Above all, words cannot express my appreciation to my mother.

ABSTRACT

THE INVESTIGATION OF DIVERSE PHYSIOLOGICAL AND THERAPEUTIC IMPACT OF CELLULAR BASED PRODUCTS DERIVED FROM HUMAN CUMULUS CELLS

The mammalian oocyte is enveloped by particular somatic cells namely cumulus cells (CCs) that support the oocyte maturation, fertility, and viability by providing the nutrients and energy. CCs have a unique extracellular matrix rich in hyaluronic acid (HA), which is responsible for the cumulus cell expansion event having a part in ovulation, fertilization, and determination of oocyte quality. At in vitro fertilization laboratories, partial removal of CCs is required to evaluate egg maturity and to have a better visualization of the oocyte during an intracytoplasmic sperm injection procedure.

In this study, discarded human cumulus tissues were used to reveal the value of HA-rich CCs. The usage of conditioned medium, recovered from the primary culture of CCs, was designed for repairing functionally distorted human nucleus pulposus cells (hNPCs) through the induction of enhanced chondrogenesis. Enlightening the impact of cumulus conditioned medium (CCM) on wound healing and angiogenesis was targeted. In line with these goals, differentiation of hNPCs into chondrocytes and osteocytes with CCM as the basal medium containing traditional differentiation agents were induced upon isolation and characterization of hCCs and hNPCs. The effects were detected by differentiation-specific cell stains and gene expression analysis. Scratch assay and tube formation assay was performed for discovering the effect of CCM on wound healing after detecting the presence of angiogenesis-related genes in hCCs.

Our results showed that cumulus cell-conditioned media promoted the chondrogenesis and osteogenesis of hNPCs. Furthermore, a significant increase in the number of branches and wound closure area was detected only in groups cultured in CCM compared to the control. Remarkably, it was shown that the hCCs can be suggested as an alternative model to the widely used models in angiogenesis assays. When all these are considered, *trashed* cumulus cells are a very special and promising cell source that should be highlighted as a *treasure*.

ÖZET

İNSAN KUMULUS HÜCRELERİNDEN TÜRETİLEN HÜCRE BAZLI ÜRÜNLERİN ÇEŞİTLİ FİZYOLOJİK VE TERAPÖTİK ETKİLERİNİN ARAŞTIRILMASI

Memeli oositi, özel somatik hücrelerden olan kumulus hücreleri (CC'ler) ile çevrelenir. Bu hücreler, oosite besin ve enerji sağlayarak oositin olgunlaşmasını, doğurganlığını ve canlılığını destekler. CC'lerin kendine özgü hücre dışı iskeletleri hyaluronik asit (HA) bakımından zengindir. HA; yumurtlama, döllenme ve oosit kalitesinin belirlenmesinde etkili olan kumulus hücrelerinin ekspansiyon olayından sorumludur. CC'ler, oositin olgunluğunun belirlenmesi ve intrasitoplazmik sperm enjeksiyonu sırasında daha iyi görüntülenmesi için in vitro fertilizasyon laboratuvarlarında kısmi olarak tıraşlanır.

Bu çalışmada, tıraşlanan kumulus dokusu HA açısından zengin CC'lerin değerini ortaya çıkarmak için kullanılmıştır. CC'lerin primer kültüründen elde edilen koşullu ortam sayesinde kondrojenez artırılarak, insana ait dejenere nükleus pulposus hücrelerinin (hNPC'ler) onarımı amaçlanmıştır. Bir diğer amaç ise; kumulus koşullu ortamının (CCM'in), yara iyileşmesi ve damarlanma üzerindeki etkisinin aydınlatılmasıdır. Bu hedefler doğrultusunda, hCC ve hNPC'lerin izolasyonu ve karakterizasyounu sağlanmıştır. Geleneksel farklılaştırma ajanları içeren CCM ile hNPC'lerin kondrositlere ve osteositlere farklılaşması uyarılmıştır. Araştırılan etkiler, farklılaşmaya özgü hücre boyaları ve gen ekspresyon analizi ile tespit edilmiştir. HCC'lerde damarlanma ile ilgili genlerin varlığı belirlendikten sonra, CCM'nin yara iyileşmesi üzerindeki etkisini keşfetmek için çizik deneyi ve tüp oluşumu deneyi yapılmıştır.

Sonuçlarımız, CCM'in hNPC'lerin kondrojenez ve osteojenez süreçlerini desteklediğini göstermektedir. Bunun yanısıra CCM'de kültürlenen gruplarda, kontrole göre damarsı tüp sayısında ve yara kapanma alanında anlamlı artış tespit edilmiştir. HCC'lerin, anjiyojenez deneylerinde yaygın olarak kullanılan modellere alternatif olabileceği dikkat çekmiştir. Bütün sonuçlar göz önüne alındığında; çöpe atılan CC'ler, çok özel, umut verici ve hazine olarak vurgulanması gereken bir hücre kaynağıdır.

TABLE OF CONTENTS

LIST OF FIGURES

LIST OF TABLES

LIST OF SYMBOLS/ABBREVIATIONS

°C	Degree centigrade
kDa	Kilodalton
mL	Mililiter
ng	Nanogram
nM	Nanomolar
µL	Microliter
µm	Micrometer
µM	Micromolar
ACAN	Aggrecan
ACTB	Beta actin
ARS	Alizarin red S
ATP	Adenosine triphosphate
BMP-2	Bone morphogenetic protein-2
BMP15	Bone morphogenetic Protein 15
CAXII	Carbonic anhydrase 12
cAMP	Cyclic adenosine monophosphate
CCs	Cumulus cells
CCM	Cumulus-Conditioned medium
CD	Cluster of differentiation
cDNA	Complementary deoxyribonucleic acid
cGMP	Cyclic guanosine monophosphate
CO_2	Carbon dioxide
COC	Cumulus-oocyte complex (COC)
Col1	Collagen type I
Col2	Collagen type II
Cox2	Cyclooxygenase 2
Cx43	Connexin-43
DMEM-HG	Dulbecco's modified eagle medium - High glucose
DMEM-LG	Dulbecco's modified eagle medium - Low glucose

DNA	Deoxyribonucleic acid
DPBS	Dulbecco's phosphate-buffered saline
ECM	Extracellular matrix
EG	Experimental group
EGF-L	Epidermal growth factor-like
ESCs	Embryonic stem cells
FBS	Fetal bovine serum
FDA	Food And Drug Administration
FOXF1	Forkhead box F1
FSH	Follicle stimulating hormone
GAG	Glycosaminoglycans
GAPDH	Glyceraldehyde-3-phosphate dehydrogenase
GC	Granulosa cells
GDF9	Growth and differentiation factor 9
GlcA	D-glucuronic acid
GlcNAc	D-N-acetyl-glucosamine
Grem1	Gremlin1
HA	Hyaluronic acid
HAase	Hyaluronidase
HABP	Hyaluronic acid-binding protein
HAS	Hyaluronan synthase
HAS2	Hyaluronan synthase 2
HCl	Hydrochloric acid
HMW-HA	High molecular weight hyaluronic acid
hNPCs	Human nucleus pulposus cells
ICAM-1	Intercellular adhesion molecule 1
ICSI	Intracytoplasmic sperm injection
IL-1β	Interleukin-1 beta
ISCT	International society for cellular therapy
IVD	Intervertebral disc
IVF	In vitro fertilization
KRT19	Keratin type I cytoskeletal 19
LH	Luteinizing hormone

Lhcgr	Luteinizing hormone/chorio-gonadotropin receptor
LMW-HA	Low molecular weight hyaluronic acid
mEF	Mouse embryonic fibroblasts
MMPs	Matrix metalloproteinases
MPF	Meiosis promoting factor
MSCs	Mesenchymal stem cells
NC	Negative control
NP	Nucleus pulposus
NPCs	Nucleus pulposus cells
NTCs	Notochord cells
PC	Positive control
PCR	Polymerase chain reaction
PGCs	Primordial germ cells
PSA	Penicillin-streptomycin-amphotericin
PTX3	Pentraxin 3
RH	Relative humidity
Q-PCR	Quantitative polymerase chain reaction
RNA	Ribonucleic acid
ROS	Reactive oxygen species
Sox9	SRY-box transcription factor 9
TGFβ	Transforming growth factor-beta
TLR	Toll-like receptors
TNF-α	Tumor necrosis factor-alpha (TNF-α)
TSG-6	TNF-stimulated gene-6
TZPs	Transzonal projections
VCAN	Versican
VEGF	Vascular endothelial growth
VEGFR1	Vascular endothelial growth factor receptor 1
VEGFR2	Vascular endothelial growth factor receptor 2
VIM	Vimentin
VWF	Von Willebrand factor
ZP	Zona pellucida

1. INTRODUCTION

1.1. CUMULUS CELLS (CCS)

1.1.1. Definition of CCs

Cumulus cells (CCs) directly surrounding the oocyte are responsible for creating a suitable environment for the development of healthy oocyte [1]. CCs are denominated by their physical appearance in the last stage of folliculogenesis that describes ovarian follicles maturation. In this stage, CCs have a fluffy cloud-like view due to their extracellular matrix production (figure 1.1.) [2].

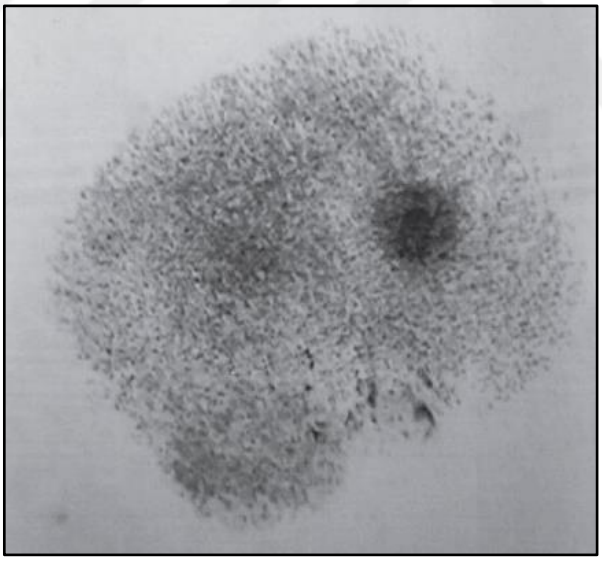

Figure 1.1. Oocyte with a cluster of CCs with ×25 magnification [3]

The tightly compact structure formed by the combination of the CCs and the oocyte is called a cumulus-oocyte complex (COC) which is consisted of 3 to 4 concentric layers of CCs. The number of CCs in these layers can be reached up to 2000 cells [4]. COC becomes clear in antral follicles and is surrounded by follicular fluid. Aspiration of this fluid, requiring for collection oocyte which is a standard step of in vitro fertilization (IVF) procedure, allows isolation of COC. In the case of intracytoplasmic sperm injection (ICSI), the next step

includes incomplete denuding of the oocyte, namely, partial removal of CCs to determine oocytes' maturity visually by the embryologist [5]. Embryologists discard some parts of CCs to determine not only oocyte maturity but also making the surface of the oocyte to be more reachable to spermatozoa by using various methods such as stripping mechanically in micropipettes, using hyaluronidase enzyme or sodium citrate [6].

1.1.2. Origin of CCs

The origin of CCs is based on undifferentiated granulosa cells (GCs) which are primary cell types in the ovary [7]. Oogenesis in mammalian begins at the embryonic period. Primordial germ cells (PGCs) constitute oogonia upon arrival to embryonic gonads-granulosa cells. At this stage, pre-granulosa cells have a flattened appearance. As the oocytes grow, the enclosing flattened pre-granulosa cells turn into cubic form to form mature GCs in primary follicles. The proliferation of GCs creates a multilayered shape and theca cells surround this structure resulting in the formation of secondary follicles. When a fluid-filled cavity inside the follicles formed, the structure called as antral follicles. At this stage, GCs differentiate into two anatomically and functionally different cell lineages, which are mural GCs and CCs by the effect of oocyte-secreted factors and ovarian hormones. Mural GCs line the follicle wall whereas CCs encircle directly oocyte [8].

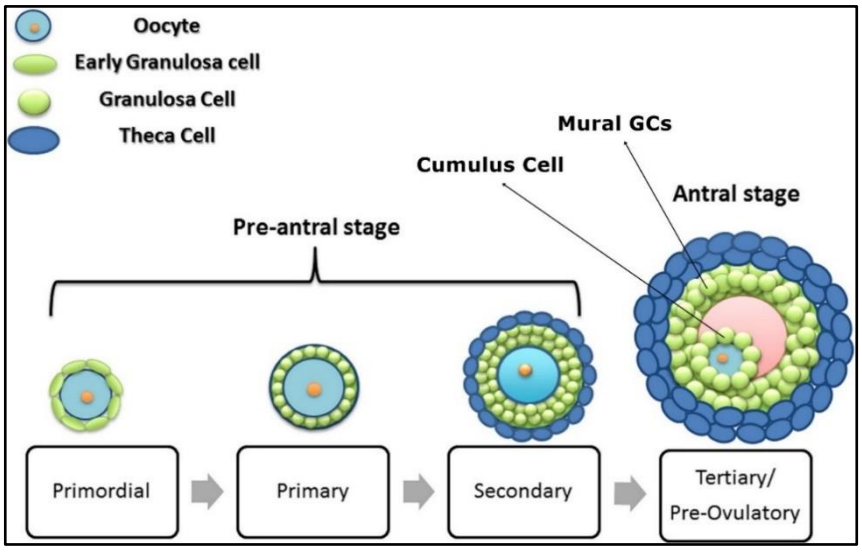

Figure 1.2. Follicle development phases in mammals [9]

Growth and Differentiation Factor 9 (GDF9) and Bone Morphogenetic Protein 15 (BMP15) secreted from oocyte play a crucial role in the differentiation of GCs and specifying of CCs [10]. Such two oocyte-specific growth factors contribute to form the cumulus gene expression profile. For instance, the expression of the Luteinizing Hormone/Chorio-gonadotropin Receptor (Lhcgr) gene in CCs is repressed by the action of GDF9 and BMP15 resulting in suppressed expression of luteinizing hormone (LH) and progesterone receptor. Because of this, compared to mural GCs, expression amount of aromatase and LH responsivity are lower in CCs. Along with these, expression of main genes unique to CCs such as enzymes taking part in glycolysis and cholesterol biosynthesis pathways are activated by signals of GDF9 and BMP15 [11].

1.1.3. Structure and Characteristics of CCs

The structure formed by thousands of CCs is called cumulus oophorus. These cells are held together by gap junctions and the unique extracellular matrix (ECM) structure. The building blocks of the gap junctions are hexamer forms of special proteins called connexins. In human cumulus cells (hCCs), connexin-43 (Cx43) is a main liable to gap junctions and is required for gaining the developmental competence of oocytes [12].

CCs have a very special ECM structure rich in hyaluronic acid (HA), which is one of the glycosaminoglycans (GAGs) and responsible for “cumulus expansion” or “mucification” that takes a role in ovulation, fertilization, or determination of oocyte quality. In more detail, ovulation of oocyte is induced by a surge of LH secreted from the pituitary gland. Due to the unresponsiveness of CCs against LH, GCs send the ovulation signal to CCs by giving a start to the production of epidermal growth factor-like (EGF-L) genes. Both EGF-L genes and follicle-stimulating hormone (FSH) provides the formation of unique ECM structure in the COCs. The important polymer HA is synthesized by the hyaluronan synthase 2 gene (Has2). HA molecules are needed for HA-binding proteins such as TNF-stimulated gene 6 (TSG6) and pentraxin 3 (Ptx3) to cross-link of HA fragments [13].

The cumulus expansion process in the last period of follicular growth is one of the crucial stages. GDF9 also plays a very important role in this phase. It coordinates enzymes in charge of CCs expansion, which creates an adequate micro-environment necessary for oocyte

development. The downstream target genes of GDF9 present in CCs and assessed as markers of oocyte developmental capacity are Has2, Ptx3, cyclooxygenase 2 (Cox2), and gremlin1 (Grem1) [14]. Likewise, these genes characterize CCs.

1.1.4. Functions of CCs

Since CCs have direct physical contact with the oocyte, they have very important roles in pre-ovulatory phases to fertilization. Transzonal projections (TZPs) with terminal gap junctions forge a link between CCs and oocyte. TZPs are thin cytoplasmic filaments allowing material transferring from CCs to the oocyte. Due to their structure, TZPs enable the passing of small molecules approximately 1 kDa [15]. These molecules can be very diverse, for instance; metabolites of glucose which are lactate and pyruvate, energy-carrying molecules, adenosine triphosphates (ATPs), cyclic adenosine monophosphate (cAMP), and cyclic guanosine monophosphate (cGMP). Ensuring the transfer of each molecule to oocyte is vital because oocytes have not sufficient glycolytic function to produce energy in the mitochondria required for metabolic activities. Since the oocyte cannot fully metabolize glucose on its own, they depend on the CCs in this pathway and the transfer of glycolysis products intercellularly [16].

In various mammals, oocytes experience two pauses during meiosis. This event is called “meiotic arrest” which is significant for reducing variances in mutations, allowing recombination of sister strands to correct genetic damage, and allaying inter-gametic conflict. A first meiotic arrest occurs at primary oocytes in prophase I stage until puberty whereas the second one appears at secondary oocytes in metaphase II until fertilization [17]. The CCs play a major role in these meiotic pauses, related to the transfer of cAMP and cGMP molecules. These cyclic nucleotides are known as second messengers in cellular pathways. A high level of cAMPs activates protein kinase-A which inhibits the function of meiosis promoting factor (MPF) by phosphorylation. This factor is one of the complex proteins involved in the regulation of the cell cycle. For the oocyte to exit meiotic arrest, MPF must be active form. The cAMPs are protected from the degradation of phosphodiesterases by cGMP. CCs elevate cAMP and cGMP levels in oocyte for the meiotic arrest. Removal of the oocyte from its cumulus cover leads to meiotic resumption because of the reduced level

of cAMP and cGMP transit to the oocyte. For second meiotic resumption, CCs again contribute to the processes by expanding their special matrix causing cAMP level fall [18].

The cumulus cells also have a specific and pivotal role in the ovulation of oocyte in tandem with the supply of metabolism and nutrients to the oocyte. For normal ovulation process, expression of cumulus-specific genes (Ptx3, Has2) and special proteins formed by GCs and integrated into COC matrices such as versican (Vcan) related with HA binding and its proteoglycanase enzyme ADAMTS1 and liver originated inter-alpha trypsin inhibitor and fetuin B are required. Hence, the COC matrix is the main ovulation mediator. Apart from these genes, some CCs-specific genes such as Grem1, Tnfaip6, and Glut4 are involved in the gaining of the developmental capability of the oocyte. This relationship is bi-directional, namely, oocyte-derived signals function on CCs to facilitate the expression of the genes and pathways necessary for sustaining oocyte growth; and the CCs feedback on complementary alimentative support [19].

At the end of the ovulation process, the function of the CCs continues. The adhesiveness of the COC matrix facilitates communication between CCs the fallopian epithelial cells. This interaction allows oocytes to travel easily through the fallopian tube to meet sperm and fertilize. COC matrix signals take a role in showing the ultimate destination to sperms. Hence, CCs have a chemoattractant role for spermatozoa. Sperms undergo capacitation and the acrosome reaction to be fertilization-capable. These sperm maturation reactions are induced by CCs and their matrix [20]. Furthermore, at the post-ovulation stage, CCs have a steroidogenic activity which leads to boost progesterone level. The hormone level changing encourages the acrosome reaction and motility of sperm. Besides, it assists to mark the egg as a target for hyper-activated sperm. The HA structure of the COC matrix is surpassed by a specific sperm protein showing hyaluronidase activity PH-20 and is important for sperm penetration to zona pellucida (ZP) [21]. Besides, the HA-rich matrix acts as a barrier for eliminating penetration of sperm with faulty hyaluronidase or motile function. HA fragments are digested by sperm-specific enzymes to reach out to Toll-like receptors (TLR) on CCs and stimulate cytokines, chemokines, and prostaglandin production. Notably, these chemokines trigger receptors on the sperm to intensify a healthy fertilization rate. Successful fertilization can be broken up the early hardening of the ZP layer which inhibits sperm

penetration. Protease inhibitors IaI and Fetuin B present in the COC matrix prohibit immature ZP hardening [22].

The other noteworthy function of CCs is protecting oocytes from the damage of higher-level reactive oxygen species (ROS) by an enabling transit of antioxidant reduced glutathione via gap junctions [23].

1.2. HYALURONIC ACID (HA)

Hyaluronic acid also termed as hyaluronan (HA) is a carbohydrate, specifically mucopolysaccharide, which is naturally present in the extracellular matrix (ECM) of various tissues or body fluids such as articular cartilage, skin, umbilical cord, and synovial fluid [24]. The first isolation of HA is performed by Karl Meyer and John Palmer in 1934 from the vitreous body of bovine's eyes [25].

1.2.1. Structural Properties of HA

HA is one of high molecular weight glycosaminoglycan comprised of repeated disaccharide building blocks. These units involve the uronic acid and aminosugar, which are D-glucuronic acid (GlcA) and D-N-acetyl-glucosamine (GlcNAc). The alternating beta-1,4 and beta-1,3 glycosidic bonds make up an unbranched non-sulfated HA structure (figure 1.3). The molecular mass of a HA unit (n) is approximately 400 kDa. The number of these units can be up to 10 000 or more [26].

In a physiological solution, the structure of HA is distinctive. Non-polarity namely relatively hydrophobic properties of HA stem from axial hydrogen atoms while side chains positioned equatorially leads to more hydrophilicity or more polarity. This situation gives rise to the formation of a twisted ribbon or coiled structure also termed as pseudorandom coil configuration [27]. Thence, a large volume of the solvent is occupied by HA. This property makes HA space-filling polymer.

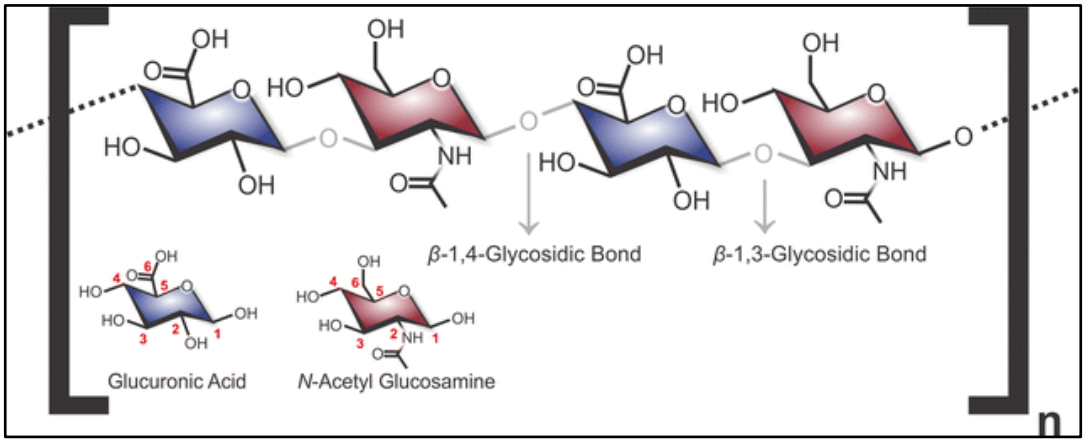

Figure 1.3. Structure of repeated disaccharide units forming HA [28]

HA has an exceptional rheological property which makes HA ideal as lubricants. In the condition of very low concentration, coil forms of HA entangle with each other whereas HA solution with higher concentrations shows extremely high viscosity, but it still depends on the shear. Another important property of HA originated from its unique structure is viscoelasticity. Intra-molecular hydrogen bonds and electrostatic repulsions between carboxylate ions (COO-) on the structure of HA contributes viscoelasticity [29].

1.2.2. HA Synthesis Strategies

Because of the biological origin of HA, synthesis at the cellular level is a highly complicated and organized process. In contrast with most glycosaminoglycans, the synthesis of HA also takes place in the plasma membrane [30].

Hyaluronan synthases (HAS) which are members of integral membrane proteins are responsible for the synthesis of this natural polymer. Three types; HAS1, HAS2, and HAS3 are found in vertebrates [31]. HAS1 is the least active form responsible for producing high molecular weight HA whereas HAS3 is the most active form generating HA with MW lower than $3x10^5$ Da. Among them, HAS2 is the main synthetic enzyme in adult cells, regulating tissue reparation, and growth [28]. The basic principle of the synthesis mechanism includes adding HA units alternately to extending the chain. In this reaction, an activated form of nucleotide sugars belonged to HA units are used as substrates.

There are several ways of HA assembling apart from the biological pathway. One of the synthesis approaches is chemo-enzymatic imitating a biosynthetic manner. The idea behind this strategy is based on using the enzyme "glycosyltransferase" which can be can be derived from a variety of organisms. Mostly, the enzyme PmHAS obtained from *Pasteurella multocida* is used to synthesize HA *in vitro* [32]. It can expand HA chains, both adding GlcA and GlcNAc blocks from the ground up and adjoining oligosaccharides of HA as acceptors. However, microbial fermentation does not enable producing the same molecular weight HA. This is a severe limitation because some functions and characteristics of HA depend on its molecular weight. For instance, HMW-HA is used to treat inflammation whereas low molecular weight (LMW)-HA has a more pro-inflammatory effect [33]. Also, the absorption properties of epithelial cells in the intestine alternates according to the molecular weight of HA. The end-product of chemi-enzymatic synthesis suffers from impurities such as microbial toxins, proteins, or nucleic acids [34].

Another HA synthesis method is the chemical approach involving two ways which are pre-glycosylation and post-glycosylation oxidation. The pre-glycosylation oxidation strategy in which GlcA units are introduced before glycosylation usually results in low to limited yields because of that GlcA units have low reactivity. This restriction makes post-glycosylation oxidation more favorable because glucose is transformed into GlcA after glycosylation. Chemical generation includes repetitive reactions such as protection, activation, coupling, and de-protection. Unfortunately, oxidation reactions of the related intermediates are highly complicated. Apart from the complex procedure, several challenges exist in chemical synthesis such as costly synthesis due to high stereo- and regio-selectivity of sugars. In large-scale production, the liberation and purification of target molecules are still difficulties [35].

1.2.3. Degradation of HA

The degradation reaction of HA occurs gradually by following chemical or enzymatic reactions and enables obtaining mono-disperse HA from the polymer form.

In the chemical method, acidic-alkaline hydrolysis is a common approach resulting in the formation of a disaccharide fragment. While the acidic environment provides cleavage of

the GlcA unit, alkaline conditions cleave GlcNAc moiety on the structure [36]. However, degradation occurs random manner, and it makes processes uncontrollable and difficult. Another HA degradation way is using ROS such as superoxide anions and hydroxyl radicals [37].

The popular trend is combining chemical and physical methodology. For instance, coupling ultrasound, copper ion, and hydrogen peroxide provides controlled degradation and leads to the formation of LMW-HA. Unfortunately, end-products are not mono-disperse. Hence, further fractionation must be applied to the products to provide homogeneity. Other physical approaches are applying heat and shear stress [38].

Enzymatic degradation can be managed by three distinct enzymes; hyaluronidase (HAase) which is derived from mammalian testes or produced as a recombinant by the microbial host, β-D-glucuronidase, and β-N-acetyl-hexosaminidase [39]. HAase is an endo-glycosidase catalyzes the reaction to generate HA oligosaccharides [40]. Likewise, microbial enzymes; HA lyases, or called chondroitin lyases are used. However, this approach needs separation with chromatography at the end because controlling the chain size of the products is challenging [41].

In brief, enzymatic or chemical processes are chosen for depolymerization reaction to produce HA oligomers. However, controlling these preparation ways is very problematic to obtain HA in pure form. Hence, the alternative ways to reach pure and structurally same HA oligosaccharides are required.

1.2.4. Applications of HA

In addition to the specific biological and chemical structure of HA mentioned before, its tissue-friendly feature creates a wide range of usage areas including food, cosmetics, pharmaceutics, and medicine depending on the size of HA and its derivatives (figure 1.4). The products containing HA is commercially available on markets. Especially, the use of HA in plenty of ophthalmic conditions such as cornea transplantation, cataract surgery, and retina-related problems is approved by the Food and Drug Administration (FDA) [42]. In plastic surgery, it is preferable as a filler also considered as “Fountain of Youth” in the

cosmetology field due to healing and moisturizing ability [43]. Some significant cell pathway-related effects are reported.

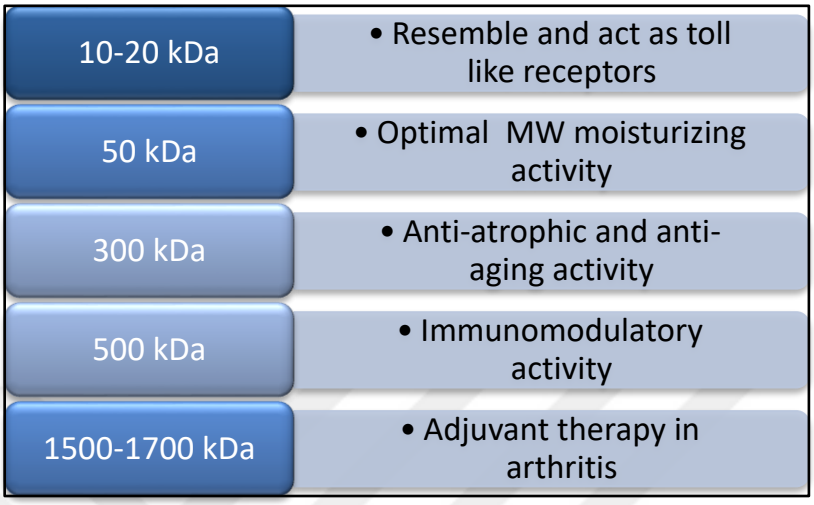

Figure 1.4. Feature of HA according to its MW [44]

1.2.4.1. Use of HA in Wound Healing and Angiogenesis

Wound healing is an innate biological process composed of three key steps; inflammatory, proliferative and re-modeling conducted by coordinated cellular actions [45]. These cellular activities are mediated by cytokines allowing the cell to generate elemental proteins and polymers needed for wound healing. One extracellular carbohydrate taking an active role in all phases of wound healing is HA.

The inflammatory, the first step of wound healing, is the phase in which HA synthesis increases swiftly. After the formation of a rift on the skin, HA fragments are produced from platelets and accessible HA in the blood circulation. HA fragments are capable of binding fibrinogen to initiate a blood-clotting pathway. Fibrinogen with its products named fibrin provides stability for local HA concentration. Massive HA releasing gives rise to saturation of the wound area with fluid causing edema which is one of the inflammation indicators. As mentioned before, due to the hydrophilic property of HA, swelling occurs at the wound site. In this situation, the porous structure forms to allow cells to migrate to the damaged area. Interleukin-1 beta (IL-1β), IL-8, and tumor necrosis factor-alpha (TNF-α) which are primary cytokines driving the inflammatory process are triggered by high concentration HA [46]. These cytokines cause the expansion of blood vessels appearing as heat and redness clinically. These symptoms decline as the inflammatory phase ends and the formation of

granulation tissue occurs for preparation of the next step of wound healing. An extension in the period of the first phase cuts-off the healing process. At that point, HA helps reduction of inflammatory symptoms by communicating with TNF-stimulated gene-6 (TSG-6) which is hyaladherin [47]. The inflammation-related protein is induced with previous inflammatory cytokines and binds HMW-HA forming heavy chains. The structure inhibits neutrophil to migrate the wound site for allaying inflammatory response.

In the proliferative phase, HA fragments having 6–20 saccharides and growth factors attract fibroblast cells toward the wound site. Fibroblast cells are in charge of constructing and holding securely newly synthesized ECM by producing collagen and GAGs involving HA. The nascent ECM has a characteristic feature as a granulated form coming from the structural property of HA [48]. Elastin and collagens elicit fibrous structure to ECM and HA provides a cushioning effect by the gel-like organization. Even though granulated tissue has elasticity, bleeding can occur due to sharp traumas. The reason for that is "angiogenesis" describing the formation of new blood capillaries. By the angiogenesis, the metabolic demands of the cells at the wound site are met. HA fragments having a short chain interact with CD44 and inducing matrix metalloproteinases (MMPs). The basement membrane of the wound is broken down by the MMPs to sprout up new capillaries from current ones [49]. Additionally, LMW-HA provides upregulation of intercellular adhesion molecule 1 (ICAM-1) having a role in forming endothelial cells [50]. This upregulation occurs indirectly depending on the expression of the inflammatory genes (TNF-α and IL-1β) in consequence of CD44 and HA interaction. However, HMW-HA decreases angiogenesis because of inhibiting early responsive genes of endothelial cells such as c-fos, c-jun, and Krox-20 [51]. Regardless, HMW-HA forming by degenerated endothelial cells rapidly turns into cleaved. Hereat, LMW-HA showing a highly angiogenic property. The last step of the proliferative phase is "epithelialization". Most of the body' HA is present in the skin at the intercellular layer which is the stratum basale of epidermis and dermis. HA has a role in hydrating stratum basale by creating channels [52]. Keratinocytes are fundamental cell groups in the basal layer and responsible for expressing CD44. Keratinocytes through the interaction of CD44 gather at wound edges and cover the wound, acting as a barricade against infections [53].

The last step of wound healing is re-modeling including scar formation by the maturation of the granulation tissue. Scarring is a foregone conclusion in wound healing because the

surface of the wound is contracted. The reason for this contraction is the differentiation of fibroblast cells taking a role in the previous phase into myofibroblast [54]. At that phase, capillary structures gather to form bigger vessels, and the content of GAGs decreases. Expectedly, HA is also degraded to provide normal scar formation.

Summing up, HA plays an important role in each phase of wound healing actively. The function of HA varies depending on its size. HMW or long HA chains act more structural roles such as creating a porous organization or filling spaces at ECM structure created by elastin and collagens, whereas LMW or small HA fragments display more stimulator and attractant characteristics such as providing migration of fibroblast and production of collagen.

1.2.4.2. Use of HA in Stem Cell Differentiation

Stem cells are prized topics in the biotechnological research area as they have a unique capability to renew themselves through a successful stream of cell divisions and differentiate into several different cell types. Such features play a central role in organogenesis during tissue regeneration and embryonic growth [55]. The promising use of stem cells to rebuild tissue and to treat a variety of previously incurable diseases inspire scientists to discover the crucial impacts of stem cell action. HA detection at certain sites where stem cells are found has increased the likelihood that HA affects these effective cells [56]. The validity of this argument has been proved by recent studies and HA which may be engineered to elicit desirable stem cell behaviors is now being investigated.

Mesenchymal stem cells (MSCs) are one of the most attractive types of stem cells as they have differentiation capacity, manipulation flexibility, and relatively simple isolation procedure. Sources of MSCs are various such as umbilical cord, synovium, bone marrow, blood, etc. [57]. To standardize MSCs' characterization, Mesenchymal and Tissue Stem Cell Committee which is a unit of the International Society for Cellular Therapy (ISCT) has established three criteria in 2006. First, MSCs must adhere to cell culture surface, and the second norm is that MSCs must express following cell surface markers CD73, CD90, and CD105 greater than 95 percent in flow cytometry analysis, whereas these cells must be deficient in expression of CD45, CD14 or CD11b, CD34, CD79a or CD19 and HLA class II. The last criterion is that MSCs must have a capacity for differentiating into osteoblasts,

adipocytes, and chondroblasts under *in vitro* differentiation conditions [58]. MSCs are intrinsically sensitive to their microenvironment as they easily respond to physical or chemical changes of their substrates or ECM. HA through various cell signaling mechanisms that comprise interactions to particular cellular receptors affects the MSCs in terms of differentiation, proliferation, and adhesion associatively. While soluble factors in cell culture medium or *in vivo* are significant stem cell differentiation regulators, recent findings have emphasized the importance of the matrix' physical and chemical features in deciding the destiny of the stem cells [59]. The studies prove the effect of HA in improved osteogenic and chondrogenic differentiation capacity of MSCs by triggering specific genes' expression. While main osteogenic markers include collagen type I (Col1), osterix, runx2, and alkaline phosphatase, chondrogenic markers are collagen type II (Col2), aggrecan, and SRY-Box Transcription Factor 9 (Sox9). The differentiation impact of HA gives an idea to scientists about designing biomaterials for the regeneration of tissues, especially bone defects. For example, in case of bone defection, commercially available HA scaffold enriched with Transforming growth factor-beta (TGFβ) made bone marrow-derived-MSCs capable of chondrogenic differentiation by generating cartilage-like structure *in vitro,* also increasing expression of chondrogenic markers. Another example includes incorporating HA-based hydrogel and morphogenetic protein-2 (BMP-2) treated-MSCs for the same intent. Again in a different study including HA-based hydrogel, osteogenic differentiation of MSCs was achieved without osteogenic medium, through the improvement of cell adhesion [60]. Additionally, the Has2 knockout mouse model has proven the significance of HA in spine development [61].

HA also enhances the differentiation behavior of embryonic stem cells (ESCs) with having pluripotency [62]. Namely, these cells can produce cell types coming from germ layers; ectoderm, mesoderm, and endoderm [63]. During the early embryogenesis of human beings, the HA contents of undifferentiated cells are highest and reduce as differentiation starts. It has been proposed that human-ESCs (hESCs) can accumulate and degrade HA by CD44 interactions, thus reorganize HA matrices which are essential for cell survival and migration [49]. ESCs usually need feeder layers for growth and maintenance of their characteristics. In the research, instead of the feeder layer which was mouse embryonic fibroblasts (mEF) with a known effect on pluripotency and differentiation, undifferentiated ESCs were tested on HA-coated surface up to a month. The experiment resulted in the same yield [64]. It appears that

HA matrices serve as a special environment for the hESCs, possibly owing to the regulating function of HA in the maintenance of undifferentiated hESCs both *in vitro* and *in vivo* conditions.

1.3. HUMAN NUCLEUS PULPOSUS (NP)

1.3.1. Location of NP Tissue

The body is mainly supported by the spine structure which is composed of vertebra defining bone segments, ligaments, and discs [65]. Two neighboring vertebral bodies are connected by the intervertebral disc (IVD). IVD makes the spine flexible without losing an abundant amount of strength and helps the movement of the body. Structurally, each disc contains three separate regions; nucleus pulposus (NP), annulus fibrosus, and cartilaginous endplates acting as a mechanical barrier and taking a role in nutrient transportation. The core component of IVD is the NP wrapped around by collagen-rich annulus fibrosus [66].

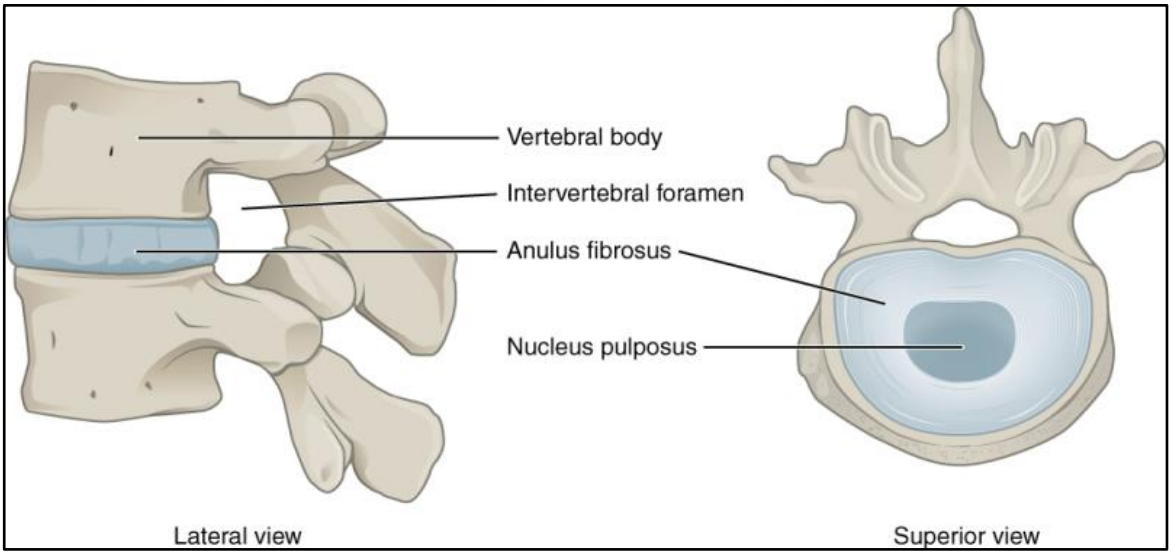

Figure 1.5. The anatomical structure of IVD [67]

1.3.2. Structure and Function of NP

The stability and flexibility of the spine are provided by the special jelly-like structure of NP. It is constituted by mostly water, sulfated-GAGs, type II collagen, and chondrocyte-like cells. These structural elements make NP elastic so it endures compression by being flexible against stress conditions. The great deal of sulfated-GAGs creates high charge density. The water absorption and swelling of NP during mechanical situations occur due to charged groups on GAG and counter ions such as sodium (Na^+). Osmatic imbalance leading to hydrostatic pressure in NP is avoided by the counterions which bring water into the tissue. This gelatinous mechanical strength helps NP to pick up the tension exerted on the spine and balance it by distributing to annulus fibrosus and the endplates [67]. Furthermore, collagen fibers organized randomly within the NP takes a role in providing tensile strength [68].

1.3.3. Origin of NPCs

Embryologically, cells of the NP derive from the notochord. Around 8-10 years of age, these cells fully turn into more chondrocyte-like characteristics. Actually, at birth, the NP tissue involves two cell types which are notochord cells (NTCs) having NP progenitors feature and nucleopulpocytes synthesizing special ECM of NP. The common cell in the NP tissue of the 26-28 week fetus is notochordal cells [69]. Notochordal cells are tightly equipped with substantial intracytoplasmic glycogen storage. Electron microscopic investigations indicate that several cell junctions link the cell membrane of these tightly packed cells. In fetal tissue, notochordal cells seem elongated form and the pericellular matrix surrounding chondrocytes is absent in these cells. Upon birth and with aging, notochordal cells lose their elongated shape, separate and transit into rounded or smaller non-vacuolated view due to fact that the special microenvironment of fully formed NP tissue does not allow the developing of cells from older notochordal cells. Additionally, an apparent pericellular matrix structure develops around it. Such new, smaller cells are prevalent type in NP at the end of the first decade of life [66].

Genetically, the expression of collagen II and aggrecan occurs in both NP cells and chondrocytes. The reason for that most common proteoglycan of NP tissue is aggrecan and

collagens constitute an important component of the NP matrix [70]. Moreover, carbonic anhydrase 12 (CAXII) has been accepted as a marker gene for characterizing human NP tissue and provides pH balance with the NP environment [71]. Also, SOX9, Forkhead Box F1 (FOXF1), and Keratin type I cytoskeletal 19 (K19 or KRT19) are other marker genes for NP cells [72]. In fetal life and childhood, NP cells express also vimentin taking role in architectural support. Also, the NP of adults contains remnants of vimentin-positive NP cells [73].

1.3.4. NP Herniation

The tear or breaking open annulus fibrosus structure leads the NP to escape from its boundaries defining as “disc herniation”. When a disc herniates, the pressure occurs on the spinal cord or spinal nerves and this situation gives rise to pain. Symptoms of a hernia are acute pain in the lower back and leg, spasm or cramping on muscles, sciatica. Some biological reflexes and physiological activities such as bending, sneezing, and coughing increase pain intensity [74]. Lifestyle choices including inadequate nutrition or absence of exercise and poor body posture trigger disk herniation. Apart from these reasons, aging causes natural structural changes at the disc. With age, IVD is less capable of tolerating shocks from body movement due to that IVD in time dehydrate and become stricter [75].

There are four stages of hernia; (1) disc degeneration occurring weak disc with aging without herniation, (2) prolapse also known as a bulging disc or a protruding disc referring changes in the position of discs which causes contact with spinal nerves, (3) extrusion which states breaking wall of annulus fibrosus by NP, however, NP is still within the disc and lastly, (4) sequestration defining go outside of NP cells from IVD disc [76]. X-ray, CT, and MRI technologies are used for the diagnosis of a hernia [77]. As a treatment, there are non-surgical and surgical options. Operations usually involve discectomy removing the abnormal disc. NP cells can be isolated for developing regenerative approaches thanks to the expression of its special genes from the operation of lumbar disc herniation. There are also unique solutions or methods to remove only the herniated disc part [78].

1.4. AIM OF THE STUDY

This study aims to elucidate the potential of cellular products derived from human cumulus cells on stem cell differentiation, wound healing processes, and angiogenesis. It is aimed to restore the cartilaginous property of human nucleus pulposus cells upon revealing their mesenchymal characteristics. The study is designed for introducing cumulus cells to scientific disciplines as a promising cell population in the treatment of intervertebral disc degeneration along with displaying their potential in enhancing wound healing processes and angiogenesis.

2. MATERIALS AND METHODS

2.1. PRIMARY CELL CULTURES

This section includes the methods of generating the primary cells used throughout the project. These cells, namely human Cumulus Cells (hCCs) and human Nucleus Pulposus Cells (hNPCs) were obtained from the parental tissues through mechanical and enzymatic digestion methods.

2.1.1. Isolation of Human Cumulus Cells (hCCs)

The tissues which were the sources of hCCs were provided by the in vitro fertilization (IVF) laboratory at Yeditepe University Hospital during the project according to the ethical principles. Primary cells were incubated in collagen type I (#07005, Stemcell Technologies, Canada) coated flasks. The coating procedure was done according to the manufacturer's instructions. Briefly, flasks were coated with 50 μg/ml collagen type I diluted in 0.01 N hydrochloric acids (HCl, #84429, Sigma-Aldrich, Germany), incubated at room temperature for 1-2 hours, and washed with Dulbecco's phosphate-buffered saline (DPBS, #14190144, Thermo Fisher Scientific, USA).

Generating the primary cells began with discarding the medium containing the tissue by centrifugation at 1300 rpm for 5 minutes. The pellet was washed with DPBS repeatedly to get rid of excessive blood residues and further digested by harsh pipetting in RPMI 1640 (#21875034, Thermo Fisher Scientific, USA) containing 10 percent (v/v) heat-inactivated fetal bovine serum (FBS, #16140071, Thermo Fisher Scientific, USA) and 1 percent (v/v) Penicillin-Streptomycin-Amphotericin B (PSA, #15240062, Thermo Fisher Scientific, USA) solution. Then, cells were transferred to collagen type I coated T25 flasks for incubation overnight under conditions of 5 percent carbon dioxide (CO_2) and 80 percent humidification at 37 °C. On alternate days, the medium of hCCs was collected, filtered with 0.22 μm filter (#FJ13ASCCA002DL01, GVS Filter Technologies, UK), and kept at -80 °C until used. The medium collection procedure continued for one week and the collected media

was named Cumulus-Conditioned medium (CCM). At the same time, cells were collected for characterization. For this, cells were washed with DPBS, detached from the flask surfaces with Trypsin-EDTA (0.25 percent, #25200056, Thermo Fisher Scientific, USA) for 5 minutes at 37 °C, and lastly centrifuged. The pellets were kept at 80 °C for further Ribonucleic acid (RNA) isolation.

2.1.2. Isolation of Human Nucleus Pulposus Cells (hNPCs)

The tissues excised from hernia surgeries were kindly obtained from Yeditepe University Hospital in accordance with ethical principles. The fluid containing the tissue was discarded by centrifugation for 5 minutes at 1300 rpm. In sterile conditions, the tissues were divided into small pieces with a scalpel and transferred to falcon tubes containing 1 ml 3 percent Pronase enzyme (#10165921001, Roche, USA) and 9 ml serum-free DMEM with low glucose (DMEM-LG, #12320032, Thermo Fisher Scientific, USA). The samples were incubated on a shaker for 1 hour at 37 °C. Later, the digestion solutions were removed by centrifugation. The tissues were treated with 1:10 collagenase (#07415, Stemcell Technologies, Canada) diluted in serum-free DMEM-LG for overnight at 37 °C on the shaker. The following day, the collagenase solution was discarded by centrifugation. After this step, the tissues were cut into smaller pieces as much as possible and placed in 60 cm^2 Petri dishes (#93100, TPP, Switzerland). Tissues pieces on the plate were fed by DMEM-LG containing 10 percent FBS and 1 percent PSA as droplets and incubated for one hour in regular cell culture conditions (5 percent CO_2, 80 percent relative humidity (RH), and 37 °C). Tissues were allowed to adhere to the surfaces and fed with higher amounts of media to grow. The tissues were kept in the petri dish until the cells explanted from them. When the cells appeared and continued to spread, tissue pieces were discarded. Upon several passages, the cells were characterized by gene expression analysis.

2.2. CHARACTERIZATION OF THE CELLS

2.2.1. Morphological Analysis

Once the cells (hCCs and hNPCs) adhered to the flask surfaces and acquired a stable morphology, images were captured under an inverted microscope (Carl Zeiss Microscopy, Germany) with various objective lenses (4X and 10X). The morphology of the cells was compared with the ones in the literature.

2.2.2. Gene Expression Characterization

Genes expressed specifically in hCCs and hNPCs were confirmed. In summary, RNAs were isolated and reverse transcribed to complementary DNA (cDNA), and amplified by Polymerase Chain Reaction (PCR) accordingly. This confirmation was performed by gel electrophoresis. The details of all the steps were described as below.

2.2.2.1. Total RNA Isolation

The cell pellets were used for RNA isolation by combining two different methods namely TRIzol lysis (#BS410A, Bio Basic, Canada) and silica column purification by NucleoSpin® RNA kit (#740955.50, Macherey-Nagel, Germany). Details of the RNA isolation steps were given in table 2.1.

Table 2.1. Outline of the RNA isolation procedure

Step No.	Procedure and Volume of Reagent	Centrifuge Conditions
1	Lysis of cell with 350 µl lysis solution	-
2	Filtrating cell lysate by using a filter column provided by the kit	11000 g, 2 min
3	After mixing the sample with 350 µl 70% ethanol, loading it to silica membrane-based column	11000 g, 1 minute
4	Removing salt from silica membrane by 350 µl membrane desalting buffer	11000 g, 1 minute

5	Digesting DNA molecules by 95 µL DNase reaction mixture	Incubation at RT for 15 minutes
6	Subsequent washing steps with provided wash buffers	11000 g, 1-2 minutes
7	Eluting RNA by 40-60 µL RNase-free H_2O	11000 g, 1 minute

Related RNAs were quantified by the spectrophotometer device (NanoDrop 1000, Thermo Fisher Scientific, USA) by checking the following parameters; concentration (ng/µl), $A_{260/280}$, and $A_{230/260}$ ratios. The concentration values of the samples were used for calculating an ideal RNA template volume for cDNA synthesis.

2.2.2.2. cDNA Synthesis

cDNA was synthesized by QuantiTect Reverse Transcription Kit (#205313, Qiagen, Netherland) as described in the manufacturer's instructions. Briefly, the reaction was composed of two steps which were genomic DNA elimination and reverse transcription. Firstly, gDNA wipeout treatment was applied to the samples for 2 min at 42°C. In the second part, template RNA was combined by reverse transcriptase enzyme, buffer (5x), and primer mix and incubated at 42 °C for 15 minutes. Upon incubation, at 95 °C for 3 minutes as a final step to inhibit the activity of reverse transcriptase enzyme, the reaction was terminated and the samples were kept at -20 °C until polymerase chain reaction (PCR).

2.2.2.3. Polymerase Chain Reaction

PCR quantifications were performed by using cDNA of hCCs templates to amplify the specific genes, which were Connexin 43 (CX43), Cyclooxygenase 2 (COX2), Hyaluronic acid synthase 2 (HAS2) and, Pentraxin (PTX3). Primer sequences of the genes were given in table 2.2.

Table 2.2. Sequences of primers used in hCCs characterization (F: forward, R: reverse)

Name of Related Gene	**Primer Sequence**	
Connexin 43 (CX43)	F	5'-TTCCTCTCTCGCCCCAC-3'
	R	5'-GGCCTAGAAAGCTTACCTT-3'
Cyclooxygenase 2 (COX2)	F	5'TTCAAATGAGATTGTGGGAAAAT-3'
	R	5'AGATCATCTCTGCCTGAGTATCTT-3'

Hyaluronic acid synthase 2 (HAS2)	F	5'- ATCCCATGGTTGGAGGTGTT-3'
	R	5'- TGCCTGTCATCACCAAAGCT-3'
Pentraxin (PTX3)	F	5'-CATCCAGTGAGACCAATGAG-3'
	R	5'-GTAGCCGCCAGTTCACCATT-3'

To carry out this reaction, FastMix Frenche PCR Kit (#25401, iNtRON Biotechnology, Korea) was used. The manufacturer's instructions were summarized in the following tables.

Table 2.3. Components and their volumes for conventional PCR

Name of Component	**Volume of Component**
Template DNA	2 µl
Primer (Forward)	1 µl
Primer (Reverse)	1 µl
Distilled water	16 µl
A total volume of reaction: 20 µl	

The reaction was performed at MyCycler Thermal Cycler (#580BR, Bio-Rad, USA). Table 2.4 shows the thermal cycler conditions applied during the reaction.

Table 2.4. Recommended thermal cycler conditions for conventional PCR

PCR Cycle	**Temperature**	**Cycle Time**	**Cycle Number**
Initial denaturation	94 °C	2 min	1
Denaturation	94 °C	20 sec	40
Annealing	60 °C	10 sec	
Extension	72 °C	50 sec	
Final Extension	72 °C	5 min	1

2.2.2.4. Quantitative-PCR (Q-PCR)

cDNA of hNPCs were used to detect hNPCs-specific genes by Taqman gene expression assay method. Since these cells have a chondrogenic origin, the presence of the chondrogenicity genes was checked for expression. Related genes and their Taqman primer-

probe (#4331182, Thermo Fisher Scientific, USA) IDs were given at the following table. Glyceraldehyde-3-Phosphate Dehydrogenase (GAPDH) was used as a housekeeping gene.

Table 2.5. Taqman primers used in Q-PCR

Name of Target Gene	**Taqman Assay ID**
GAPDH	Hs02786624_g1
Vimentin (VIM)	Hs00958111_m1
SRY-Box Transcription Factor 9 (SOX9)	Hs01001343_g1
Aggrecan (ACAN)	Hs00153936_m1
Forkhead Box F1 (FOXF1)	Hs00230962_m1
Carbonic Anhydrase 12 (CA12)	Hs01080909_m1
CD44	Hs01075864_m1
Beta-Actin (ACTB)	Hs01060665_g1
Cytokeratin 19 (CK19)	Hs00761767_s1

The assay was done by using Promega Taqman master mix (#A6121, Promega, USA). The table shows the components of the reactions.

Table 2.6. Components and their volumes for Q-PCR

Name of Component	**Volume of Component**
GoTaq Probe Master Mix	5 µl
Primers	0.4 µl
Template DNA	2 µl
Nuclease-Free Water	2.6 µl
A total volume of the reaction: 10µl	

This experiment was conducted in the CFX96® Real-time PCR system (Bio-Rad, USA). For thermal cycling conditions, the manufacturer's instructions were based on. The below table is outlined advised protocol.

Table 2.7. Recommended thermal cycler conditions for Q-PCR

PCR Cycle	Temperature	Cycle Time	Cycle Number
Initial denaturation	95 °C	2 min	1
Denaturation	95 °C	15 sec	40
Annealing/Extension	60 °C	1 min	

2.2.2.5. Gel Electrophoresis

To monitor and detect the related gene expressions, gel electrophoresis was performed by preparing 2 percent agarose gel (#1012360100, Sigma Aldrich, USA) in 100 ml Tris-Borate-EDTA (TBE, #93290, Sigma Aldrich, Germany) buffer. Until obtaining a homogenous solution, the gel solution was heated in a microwave. To make cDNA bands visible under UV light, 3.5 µl ethidium bromide (EtBr, #15585011, Thermo Fisher Scientific, USA) was added to the prepared solution. Upon the gel polymerization, the end products from the conventional PCR were loaded to the wells of the gel by mixing with 6X loading dye (#B7024S, New England Biolabs, USA) for tracking the samples. Electrophoresis was run through at 100 volts for 45 minutes (Bio-Rad, USA). The images of the gels were captured by a gel documentation system (Gel Doc XR$^+$, Bio-Rad, USA)

2.2.3. Stem Cell Surface Marker Characterization of hNPCs

To determine the stem cell characteristics of hNPCs, specific surface proteins were detected and analyzed by flow cytometry. The pellet of hNPCs was collected as described in section 2.1.2. The pellets were washed once with DPBS and resuspended with 2 percent paraformaldehyde (PFA) for the fixation procedure. The samples were incubated at +4 °C for 30 minutes. After the incubation, PFA was discarded by centrifugation at 1300 rpm for 5 minutes. The samples were washed once again and resuspended in 1100 µl DPBS. The fixed pellets were dispensed into 11 tubes and one tube for control. Designated antibodies were added to the tubes as the manufacturer's recommended amount. The conjugated antibody used was purchased from the Abcam (UK) and the list is as follows; CD31, CD14, CD34, CD45, CD117, CD29, CD73, CD44, CD90, and CD105. The samples with various antibodies were incubated at +4 °C overnight in dark. The following day, samples were washed once to remove the excess of antibodies. Samples were then transferred to the flow

tubes labeled for each antibody and analyzed in appropriate channels (FL1 and FL2) using BD FACSCalibur™ (Becton Dickinson, USA).

2.2.3.1. CD105 Expression Analysis

As described earlier in the previous sections (2.1.2 and 2.2.3), the hernia tissues taken from four different patients were prepared for flow cytometry analysis. The data that belonged to CD105 were analyzed in detail.

2.2.4. Angiogenic Marker Characterization of hCCs

To determine the angiogenic potential of hCCs, the genes expression analysis was performed as described in 2.2.2. The sequences of angiogenic primers used for PCR were given below. 18S primer was used as a housekeeping gene during the assay.

Table 2.8. Sequences of primers used in the angiogenic characterization

Name of Related Gene	Primer Sequence	
18S	F	5'-GTAACCCGTTGAACCCCATT-3'
	R	5'-CCATCCAATCGGTAGTAGCG-3'
Vascular endothelial growth factor (VEGF)	F	5'-TTGCCTTGCTGCTCTACCTC-3'
	R	5'-AGCTGCGCTGATAGACATCC-3'
Vascular endothelial growth factor receptor 1 (VEGFR1)	F	5'-CAGGCCCAGTTTCTGCCATT-3'
	R	5'-TTCCAGCTCAGCGTGGTCGTA-3'
Vascular endothelial growth factor receptor 2 (VEGFR2)	F	5'-CCAGCAAAAGCAGGGAGTCTGT-3'
	R	5'-TGTCTGTGTCATCGGAGTGATATCC-3'
Von Willebrand factor (VWF)	F	5'-CGGCTTGCACCATTCAGCTA-3
	R	5'-TGCAGAAGTGAGTATCACAGCCATC-3'

2.3. CELL VIABILITY ASSAY

Throughout the project, as the CCM will be applied to the hNPCs, the highest but non-toxic dose of CCM that should be given to the cells was determined by 3-(4,5-Dimethylthiazol-2-

yl)-5-(3-carboxymethoxyphenyl)-2-(4-sulfophenyl)-2H-tetrazolium (MTS, #G1111, Promega, USA) assay. Shortly, hNPCs were seeded onto the 96-well plates (#CLS6509, Corning, USA) at a density of $5x10^3$/well. The plates were placed under regular cell culture conditions for overnight to allow the cells to adhere. After 24 hours, hNPCs were treated with CCM diluted with normal culture medium of hNPCs (DMEM-LG containing 10 percent FBS and 1 percent PSA) at a 1:1 ratio. The normal medium used in CCM dilution was also given to the cells as a control group. To determine the effect of CCM on cell viability, four different time points (24, 48, 72, and 96 hours) were selected. At every time point, 10 percent MTS reagent prepared in 0.45 percent glucose in DPBS solution (#G8644, Sigma Aldrich, Germany) was applied to the wells. The plates were incubated in a humidified chamber (5 percent CO_2, 80 percent RH, and 37 °C) for 1 hour in dark. Absorbance values of end-products of the reaction were determined by a plate reader (ELx800, Biotek Instruments, USA) at wavelength 490 nm. Lastly, results were analyzed by comparing CCM diluted at a 1:1 ratio with the control group.

2.4. HYALURONIC ACID (HA) QUANTIFICATION IN CCM

The amount of hyaluronic acid in the CCM was determined by the ELISA-like assay for HA (#AMS.CSR-HA-96KIT, Amsbio, USA). Firstly, wells were coated with HA coating solution and incubated for 1 hour. After washing the wells with the wash buffer, the blocking buffer was added and incubated for 30 minutes. After following the wash processes again, standards, samples including many CCM mixes, and RPMI-1640 containing 10 percent FBS control were added to the treated wells as duplicate. Biotin-Hyaluronic acid-binding protein (HABP) was added and incubated for 1 hour. HRP-Avidin was introduced to each well and incubated for 1 hour. The wells were thoroughly washed, substrate solution was applied, and the plate was incubated for 30 minutes in dark. The stop solution was added to each well lastly. The absorbances were measured at 450 nm wavelength using the plate reader immediately. The calibration curve was plotted against the absorbances of standards and the concentrations of HA in CCMs were determined.

2.5. CHONDROGENIC DIFFERENTIATION

To observe the effect of CCM on chondrogenic differentiation, hNPCs were induced with differentiation agents as given in table 2.9 [79]. The droplet culture method was applied to mimic three dimensional (3D) environment for cells. Shortly, hNPCs were seeded at a density of 200 000 cells/50 µl to the center of the wells as a droplet and incubated in the humidified chamber approximately 1-2 hours. Upon incubation, cells were treated with specific culture media stated in table 2.10. Cells were grown in the culture for 21 days for the completion of the differentiation with refreshed media three times a week. The differentiation medium was prepared freshly every week.

Table 2.9. Differentiation agents for chondrogenesis

Name of Chemical	**Concentration**
Dexamethasone (#DEX002.50, BioShop, Canada)	100 nM
L-Ascorbic acid (#A4544-25G, Sigma-Aldrich, Germany)	50 µg/ml
L-Proline (#PRO222.25, BioShop, Canada)	40 µg/ml
Sodium-Pyruvate (#600-110-EL, Wisent Bioproducts, Canada)	10 µg/ml
Transforming growth factor-beta (TGF-β, #100-21C, PeproTech, USA)	10 ng/ml
Insulin-Transferrin-Selenium (ITS, # 41400045, Thermo Fisher Sci., USA)	1% (v/v)

Table 2.10. Groups designed in the chondrogenic differentiation

Name of Group	**Differentiation Agents**	**Medium**	**FBS**	**PSA (1 %)**
Negative Control (NC)	-	DMEM-LG	+ (10 %)	+
Positive Control (PC)	+	DMEM-HG	-	+
Experimental Group (EG)	+	DMEM HG – CCM (1:1)	-	+

2.5.1. Morphological Analysis

At the end of 21 days, the images of morphological changes in hNPCs were taken under the inverted microscope (Carl Zeiss, Germany). Spreading of the cells from the droplets were captured and compared among the groups.

2.5.2. Alcian Blue Staining

To determine the chondrogenic differentiation, cells were stained with the alcian blue stain. Alcian blue staining enables the detection of acid mucosubstances and acetic mucins, which are the indicators of chondrogenicity. For preparing the stain solution, 1 gram alcian blue powder (#A9186, Sigma-Aldrich, Germany) was dissolved in 100 ml 3 percent acetic acid (#33209, Honeywell Riedel-de-Haën, Germany). The solution was filtered with a 0.45 μm filter (GVS Filter Technologies, UK). Cells were fixed with 4 percent PFA for 30 minutes at +4 °C. After fixation, cells were washed with DPBS for three times. The staining solution was added to wells and incubated for 30 minutes at RT in dark. Lastly, the wells were washed three times. After the staining was completed, the images of the wells were captured. The average blue color intensity in the images was analyzed by the ImageJ image processing program developed at the National Institutes of Health (USA).

2.5.3. Gene Expression Analysis

Chondrogenic differentiation was also evaluated by quantifying the gene expression levels, which were specific to chondrogenesis. According to the Q-PCR analysis, fold changes in collagen type II alpha-1 gene (COL2A1) which is a main marker of chondrogenesis were determined and compared among the groups by using the statistics software (GraphPad Software Inc., USA). Q-PCR was performed by SYBR Green chemistry (#1901521, Thermo Fisher Scientific, USA). For thermal cycler and reaction conditions, the manufacturer's instructions were followed. The sequence of COL2A1 primer was as follows; 5'-TCTGTGTCCTCTCTTACTCTCC-3', and 5'-GGCATCTGACCTCACCAATTA-3'. The 18S was used as a housekeeping gene whose sequence was given previously.

2.6. OSTEOGENIC DIFFERENTIATION

To determine the effect of CCM on osteogenesis, hNPCs were differentiated into osteoblasts by stimulating with differentiation agents given at table 2.11 [80]. hNPCs were seeded onto six-well plates at a density of 75 000 cells/well. Cells were treated with specific culture media stated in table 2.12 and incubated for 14 days with media refreshing three times a week. The differentiation medium was prepared freshly every week.

Table 2.11. Differentiation agents for osteogenesis

Name of Chemical	**Concentration**
Dexamethasone	100 nM
β-Glycerophosphate disodium salt hydrate (#G9422-10G, Sigma-Aldrich, Germany)	10 mM
L-Ascorbic acid	50 µg/ml

Table 2.12. Groups designed in the osteogenic differentiation

Name of Group	**Differentiation Agents**	**Medium**	**FBS (10%)**	**PSA (1 %)**
Negative Control (NC)	-	DMEM-LG	+	+
Positive Control (PC)	+	DMEM-LG	+	+
Experimental Group (EG)	+	DMEM LG – CCM (1:1)	+	+

2.6.1. Morphological Analysis

After two weeks of differentiation, the images of morphological changes in hNPCs were captured under the inverted microscope. Osteoblast structures formed at differentiated groups were observed and compared among the groups.

2.6.2. Alizarin Red S (ARS) Staining

To detect calcium deposition in the cells, ARS staining was performed. The medium of the cells was discarded and the wells were washed with DPBS gently. The cells were fixed with absolute ethanol (#920.026, Isolab, Germany) for 30 minutes at RT. After the fixation, ethanol was discarded and wells were allowed to dry completely. ARS solution (#CM-0058, Lifeline Cell Technologies, USA) was introduced to the wells. The plate was incubated for 15 minutes at RT. The wells were rinsed with distilled water (dH_2O) three times.

For quantifying the staining, a leaching solution containing 20 percent (v/v) methanol (#947.043, Isolab, Germany) and 10 percent (v/v) acetic acid in dH_2O was prepared. This solution was applied to the wells for 15 minutes for extracting the ARS stain. Lastly, the absorbance of the samples was measured at 450 nm by a plate reader.

2.6.3. Gene Expression Analysis

Osteogenic differentiation was also evaluated by measuring the gene expression levels which were specific to osteogenesis for three weeks. According to the Q-PCR analysis, fold changes in osteopontin (OPN) which is a main marker of osteogenesis was determined and compared among the groups by the Graphpad Prism software. The sequences of osteopontin (OPN) primer was as follows; 5'-AGTGTAGAAGTCGGGAAGGA-3', and 5'-CAGAGACCCAGAGAACCAAAG- 3'. The 18S was used as a housekeeping gene whose sequence was given previously.

2.7. SCRATCH ASSAY

This assay was performed to make an inference about the effect of CCM on wound closure by the quantification of cell migration rates [81]. Human immortalized keratinocytes (HaCat, #300493, DKFZ, Heidelberg) were seeded onto six-well plates at 90 percent confluency. The following day, the medium was discarded and the wells were washed with DPBS very gently to make sure not to remove the cells from the surfaces. By using a sterile tip, a scratch was made in the center of the well. Floating cells upon the scratch were removed by washing

the wells once with DPBS and CCM at a 1:1 ratio was introduced to the cells. The effect of CCM was compared with the control group (regular culture medium without CCM) by taking images every six hours starting from 0-time point to 12 hours in total. Determination of the effects on wound closure was evaluated with Wimasis image analysis program (Wimasis, Spain).

2.8. TUBE FORMATION ASSAY

The tube formation assay was performed to determine the effect of CCM and hCCs on vascularization. In the assay, the effect of these groups was compared with human umbilical vein endothelial cells (HUVECs, #CRL-1730, ATCC, USA), which are known to be the established model in tube formation. Briefly, pre-chilled 48-well plates and tips were used. The plates were coated with Matrigel (#354248, Corning, USA), which was previously incubated at 4°C before the experiment. Upon polymerization at 37 °C, HUVECs and hCCs were seeded onto Matrigel-coated wells at a density of 70 000 cells/well as duplicate. The cells were treated with two different media and incubated at the humidified chamber for 5-7 hours [82]. After incubation time, images of each group were captured by using an inverted microscope. Analysis of branch numbers in obtained images was done by an image analysis program, Wimasis.

2.9. STATISTICAL ANALYSIS

Experiments were carried out in triplicate to enable a proper statistical analysis. GraphPad Prism 7.0 program was used for multiple comparisons among the experimental and control groups. One-way analysis of variance (ANOVA) with Tukey's post-hoc test was applied to data to determine the significance of differences. The $*P<0.05$ was chosen as statistically significant.

3. RESULTS

3.1. CHARACTERIZATION OF HCCS

HCCs were isolated successfully from the parental tissue by mechanical digestion. The morphologies were observed and gene expressions specific to cumulus cells along with angiogenic markers were verified to ensure whether desired cells were generated.

3.1.1. Morphology of hCCs

CCs were isolated from the tissue surrounding the oocytes collected for in vitro fertilization processes. Figure 3.1. demonstrated oocytes with cumulus cells' layers before the removal of cumulus tissue which is required for spot-on intracytoplasmic sperm injection. The oocytes were located in the center and the cumulus cells formed a puffy layer around those oocytes.

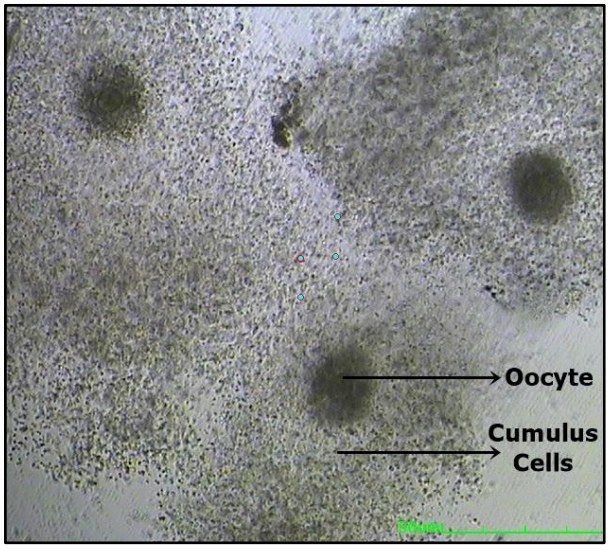

Figure 3.1. The image taken at the IVF laboratory shows the CCs surrounding the oocytes

HCCs were monitored under an inverted microscope for a week and the morphology of the cells was saved. The images of the cells in the early days of culture and the days before harvest were captured as shown below.

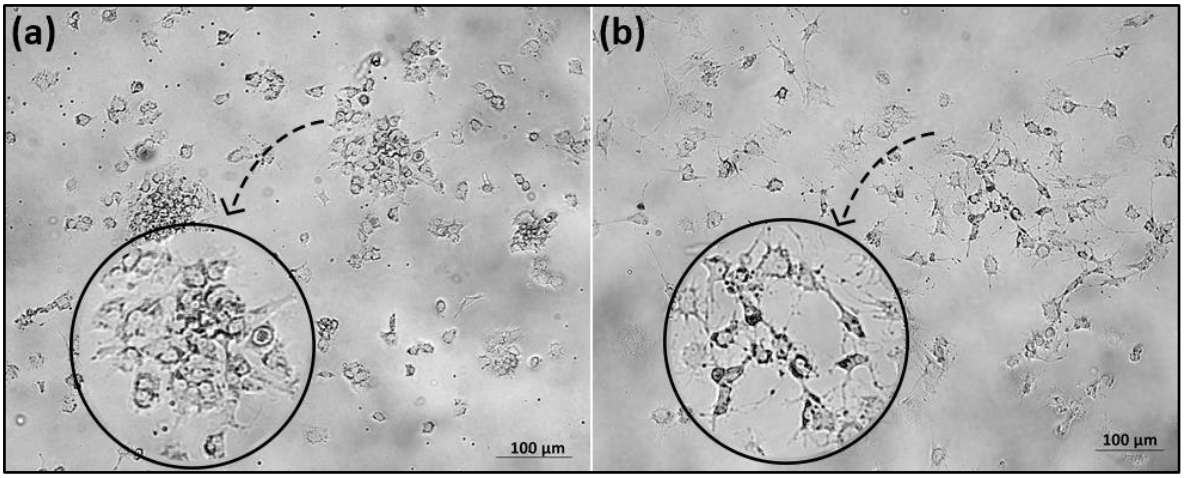

Figure 3.2. hCCs at (a) early days (1-3 days), (b) late days (4-7 days). Scale bar: 100 µm

In the early days, hCCs were small and rounded but they transition into a different look as time progresses and gain spindle-shaped with growing arms, probably creating junctions. At the end of the week, the senescent period of hCCs began. During this period, the spindles disappeared, the cells became larger and their morphology was distorted as seen in Figure 3.3.

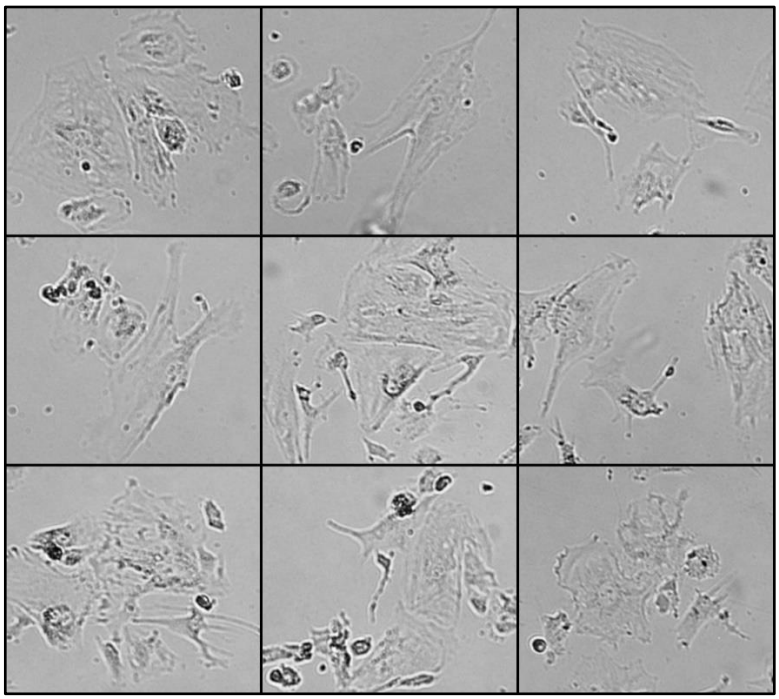

Figure 3.3. hCCs randomly captured from the population after 7 days of the culture

3.1.2. Gene Expression of hCCs

Genes specific to hCCs were amplified and analyzed with gel electrophoresis. The expressions were demonstrated in figure 3.4.

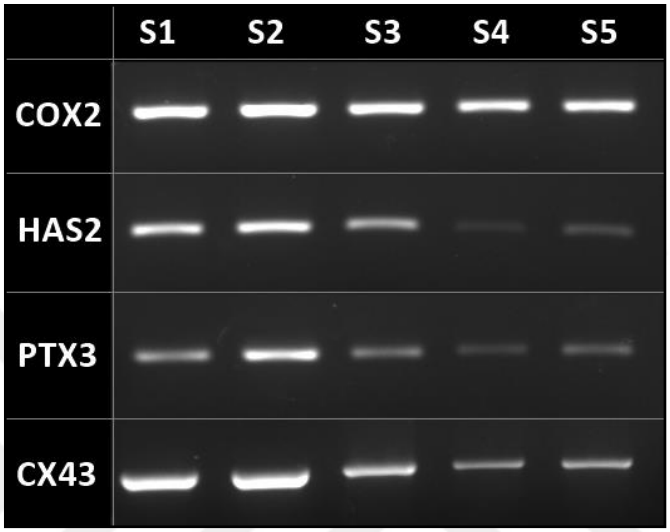

Figure 3.4. Gene expressions of hCCs from five parental tissues. “S” represents “Sample”

According to figure 3.4, the expression levels of genes generally varied from sample to sample. For instance, Has2 and Ptx3 expression levels in sample 2 (S2) were the highest whereas sample 4 (S4) had the lowest one. On the other hand, the Cox2 expression level was the most consistent among them. These inferences were based on the brightness of the bands and they are all considered cumulus positive. Due to the various gene expression levels of five patients, it was decided that CCM obtained from each patient of primary cumulus cells were mixed.

3.1.3. Angiogenic Markers of hCCs

Angiogenic markers namely VEGF, VEGFR1, VEGFR2, and VWF were confirmed by gene expression analysis for the characterization of hCCs. According to results in figure 3.5, cells from different parental tissue were positive to angiogenesis markers. VEGF and VEGFR2 expressions were well, while VEGFR1 and VWF expressions were relatively low.

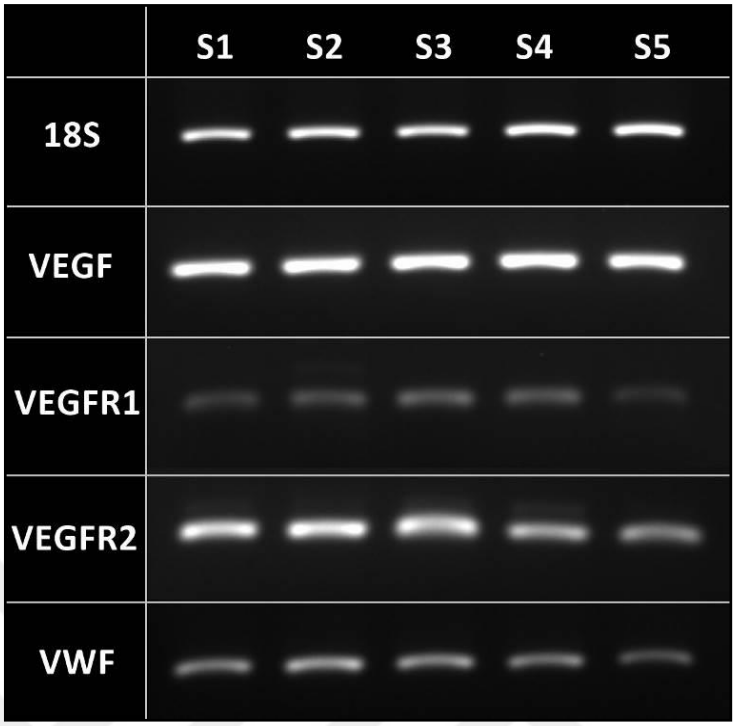

Figure 3.5. Angiogenesis-specific genes of hCCs from different parental tissues

3.2. CHARACTERIZATION OF HNPCS

HNPCs were isolated through the enzymatic methods. The characterization of the cells was provided by the morphological analysis as well as gene expression profiling. In addition to these, mesenchymal stem cell properties of the cells were also detected by flow cytometry.

3.2.1. Morphology of hNPCs

Upon the isolation, hNPCs were cultured in a sustained period and their morphologies were examined under the inverted microscope regularly. The images of the cells were displayed in Figure 3.6. According to morphologic observations, hNPCs were giant and fusiform-shaped and have a homogenous structure.

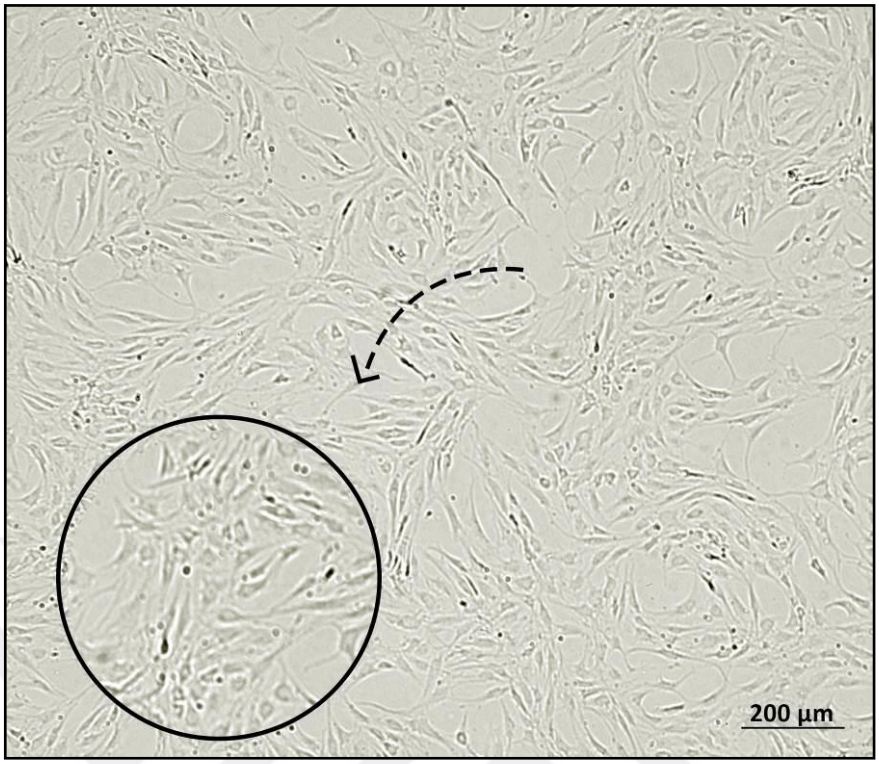

Figure 3.6. Microscopic images of hNPCs. Scale bar: 200 µm

3.2.2. Gene Expression of hNPCs

Genes specific to hNPCs, chondrification, and other mesenchymal markers including SOX9, AGGRECAN, CD44, VIMENTIN, FOXF1, CK12, and CA12 were analyzed by Q-PCR detection. Gene quantification was visualized under UV light (Figure 3.7.) and according to it, the genes were found to be expressed by the hNPCs.

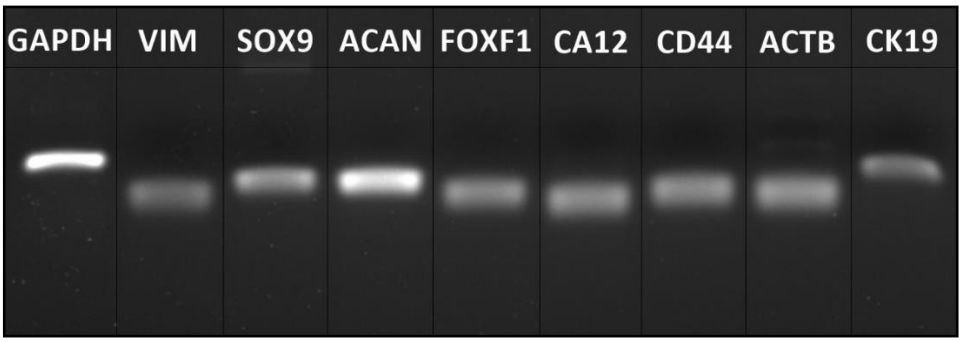

Figure 3.7. Gene expressions specific to hNPCs

While cells expressed Aggrecan in a higher amount, other genes seemed to be the less. However, all the genes that were expressed affirmed that the isolated cells were hNPCs.

3.2.3. Stem Cell Surface Markers of hNPCs

HNPCs were further characterized by the presence of mesenchymal potential. Flow cytometry analysis showed that the cells possessed mesenchymal surface markers while not the hematopoietic ones. Flow cytometry optimization of negative control, which was deficient in antibody treatment, is accessible in appendix A.

Table 3.1. Summary of the flow cytometry analysis of hNPCs

Negative Markers	
Marker Name	**Gated %**
CD31	0.90
CD14	0.83
CD34	1.37
CD45	1.06
CD117	1.32
Positive Markers	
Marker Name	**Gated %**
CD29	99.92
CD44	100.00
CD73	99.77
CD90	98.40
CD105	20.84

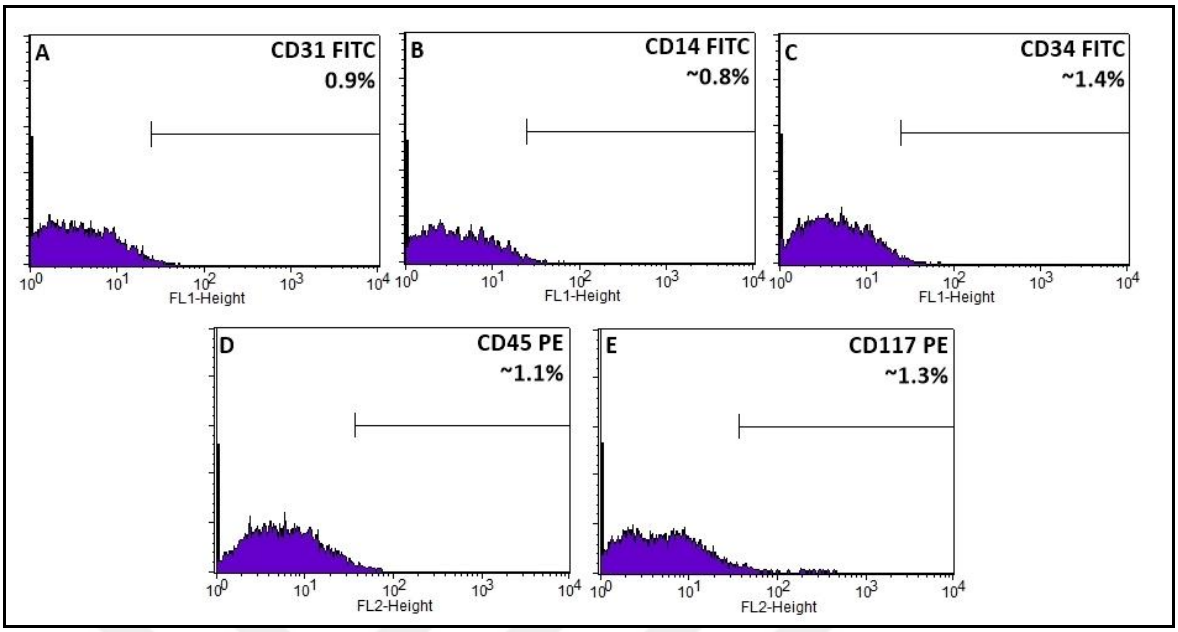

Figure 3.8. Flow cytometry analysis of hematopoietic surface markers for hNPCs

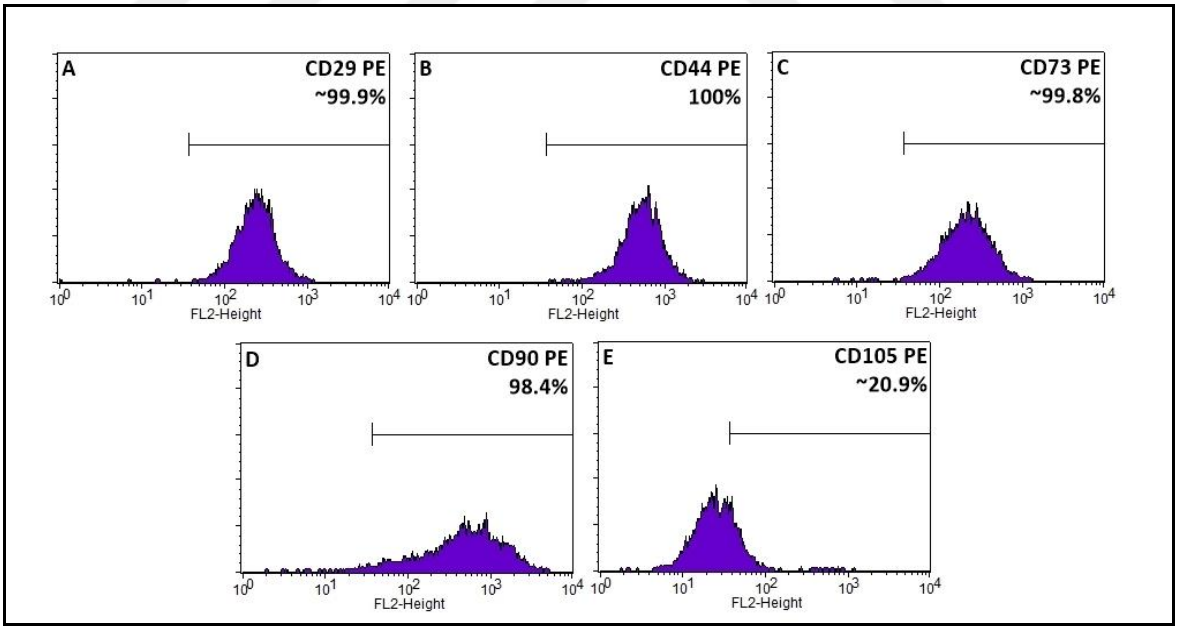

Figure 3.9. Flow cytometry analysis of mesenchymal surface markers for hNPCs

According to the analysis, hNPCs had a mesenchymal potential while they were hematopoietic negative, and were considered to have a mesenchyme origin. Surprisingly,

the CD105 expression level was low in hNPCs. To generalize the expression level of CD105, cells were isolated and characterized from four different nucleus pulposus tissue sources. Further investigation of the presence of CD105 expression demonstrated that all four of the cells had less than fifty percent CD105 expression levels as follows; 19.12, 20.84, 16.09, and 25.78 percentages respectively.

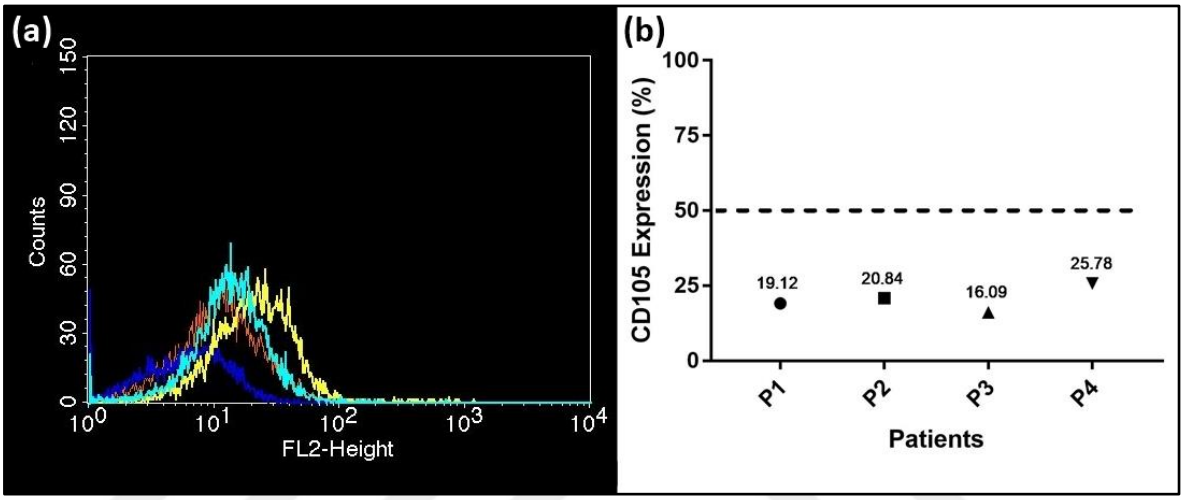

Figure 3.10. Detailed analysis of CD105 expression in four different samples. (a) Flow cytometry analysis, each color represents different samples, (b) Expression percent analysis of the same samples.

3.3. CYTOTOXICITY ASSAY

The toxicity of CCM dilution at a 1:1 ratio on hNPCs was investigated by MTS assay. It was observed that there was no significant difference in viability between the CCM (1:1) treated and untreated control groups of hNPCs for four days. CCM (1:1) dilution did not hold any toxic effect on hNPCs. Based on this result, a 1:1 dilution ratio was used in the rest of the assays.

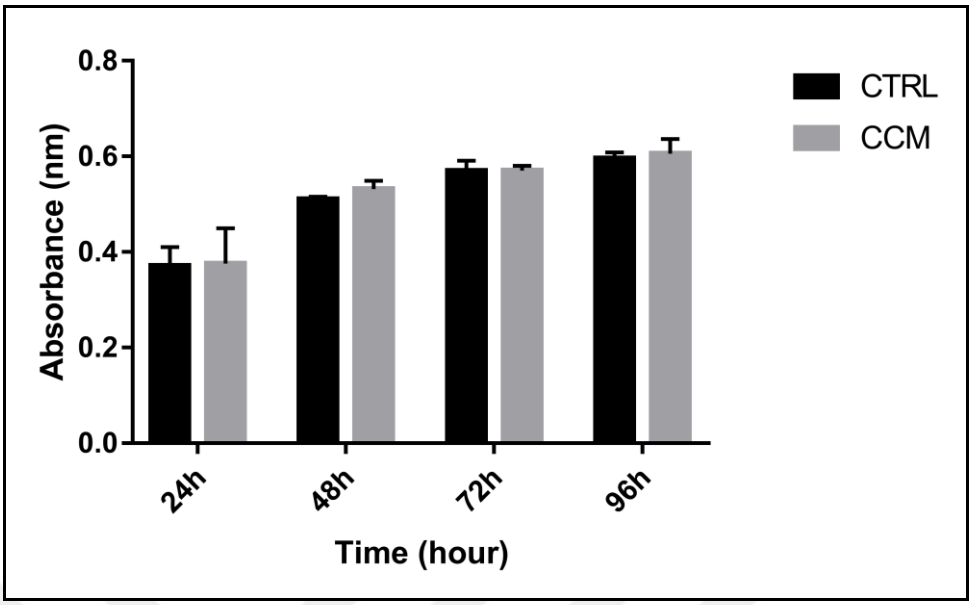

Figure 3.11. Cell viability assay showing an effect of CCM dilution at 1:1 ratio versus the control group (DMEM-LG) on hNPCs' viability

3.4. HYALURONIC ACID (HA) QUANTIFICATION IN CCM

To detect the hyaluronic acid amount in CCM, an ELISA-like assay was carried out. The basal culture medium of hCCs namely RPMI was used as a negative control whereas RPMI with 10 percent FBS was used as a positive control in the assay.

According to the results given in figure 3.12, CCM consisted of a high amount of HA; 102,8 ng/ml. Compared to the positive group (RPMI with FBS), it was seen that CCM contained approximately twice as much hyaluronic acid. The calibration curve of the assay was given in appendix B.

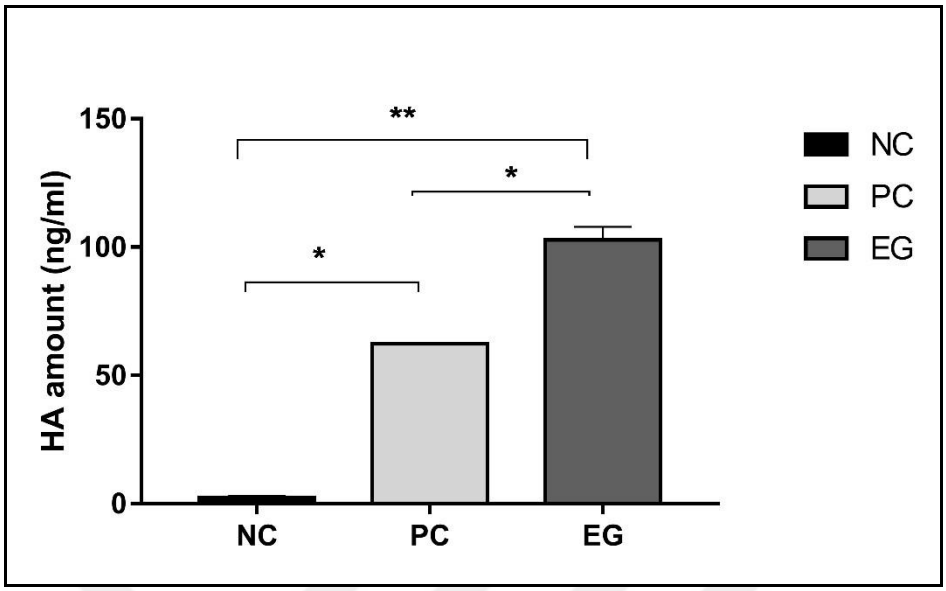

Figure 3.12. Hyaluronic acid quantification, the comparison of HA amount (ng/ml) between the experimental group (EG; CCM) and control groups, * $p < 0.05$

3.5. CHONDROGENIC DIFFERENTIATION DETECTION

Upon stimulation of chondrogenesis, conformational tests including, alcian blue staining, and detection of COL2A1 expression were performed. A morphological comparison between differentiated and undifferentiated cells was also monitored.

3.5.1. Morphological Analysis

Chondrogenic differentiation was carried out as in the droplet form. At the end of 21 days, cells' expansions around the droplet were examined. Results showed that untreated cells failed to maintain inside the limits of the initial droplet form. Cell proliferation continued around the droplet and the cells managed to leave out of the droplet However, the differentiated cells stayed inside the droplet. The growth of the cells slowed down and the spread to the outside of the droplet decreased. In the experimental group, the cells almost completely stopped falling out of the droplet. The images of all groups were shown in Figure 3.13.

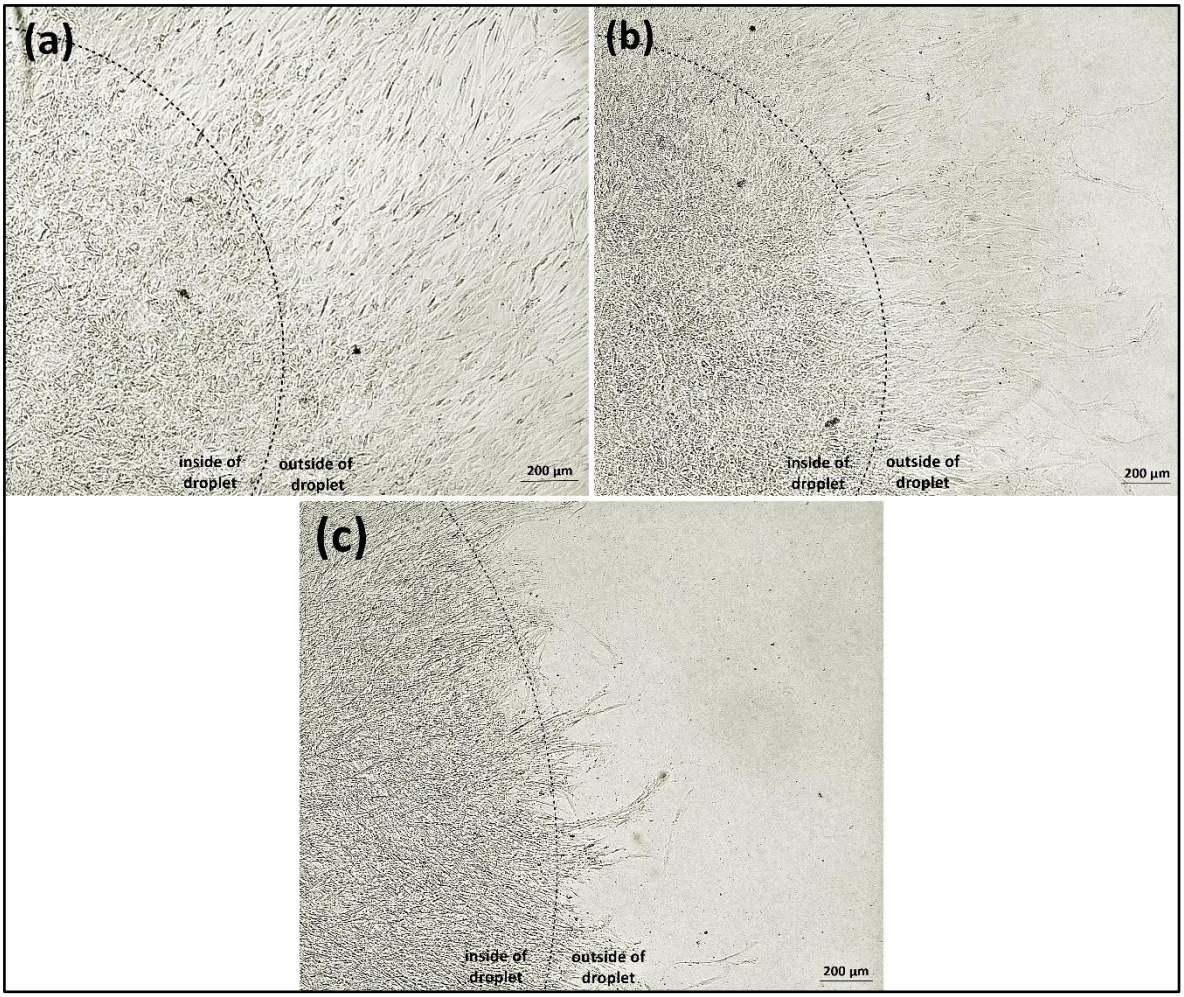

Figure 3.13. Morphological changes upon chondrogenic differentiation of hNPCs on the 21st day. (a) Negative Control, (b) Positive Control and (c) Experimental Group

3.5.2. Alcian Blue Staining Analysis

Alcian blue staining was performed to detect the presence of sulfated glycosaminoglycans, the indicators for chondrogenesis at its higher level. As seen in Figure 3.13, the most intense color of blue was observed in the experimental group whereas the lowest intensity of the blue color was detected in the untreated group. To quantify the intensity of blue color, ImageJ was made of use. Quantitative results were consistent with the observations. The intensity of blue corresponded to 6 percent in the positive control, while it reached up to 32 percent in the experimental group as shown in Figure 3.14 (a-b).

3.5.3. COL2A1 Gene Expression

COL2A1, the main protein found in cartilage structures, was examined as a marker of chondrogenesis by Q-PCR. According to the positive control, a 3-fold difference was detected in the EG as shown in Figure 3.14 (c).

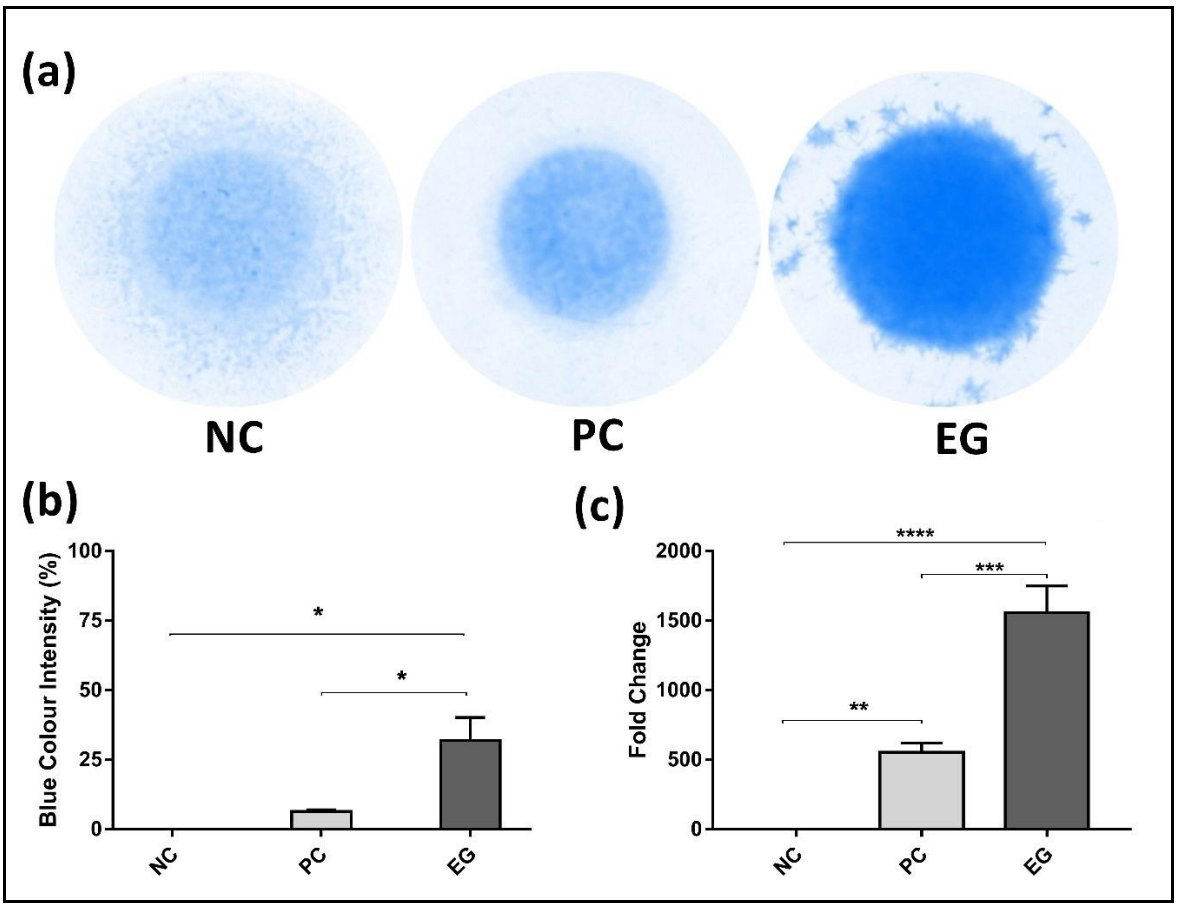

Figure 3.14. Chondrogenic differentiation data. (a) Alcian blue staining of hNPCs upon differentiation for 21 days, (b) Quantitative analysis of alcian blue staining, (c) Q-PCR analysis of the COL2A1 gene expression, * $p < 0.05$

3.6. OSTEOGENIC DIFFERENTIATION DETECTION

Both qualitative and quantitative tests were applied to determine the osteogenic differentiation. Additionally, morphology changes were observed and Alizarin Red S staining was performed.

3.6.1. Morphological Analysis

Upon the completion of osteogenic differentiation, the morphology of the cells was observed and the comparison between the groups was made. According to the observations, the untreated cells had fusiform shapes whereas, the differentiated cells gained more osteocyte-like round shapes. The number of rounded cells was higher in the EG (figure 3.15).

3.6.2. ARS Staining Analysis

ARS staining was performed to determine the calcification in the samples. As given in Figure 3.17., redness caused by the increased calcification was highest in the experimental group. The quantitative analysis also confirmed the observations. Extracting the ARS stain and measuring its absorbance allowed quantitative analysis. A 1.5-fold difference was observed between the positive control and the experimental group.

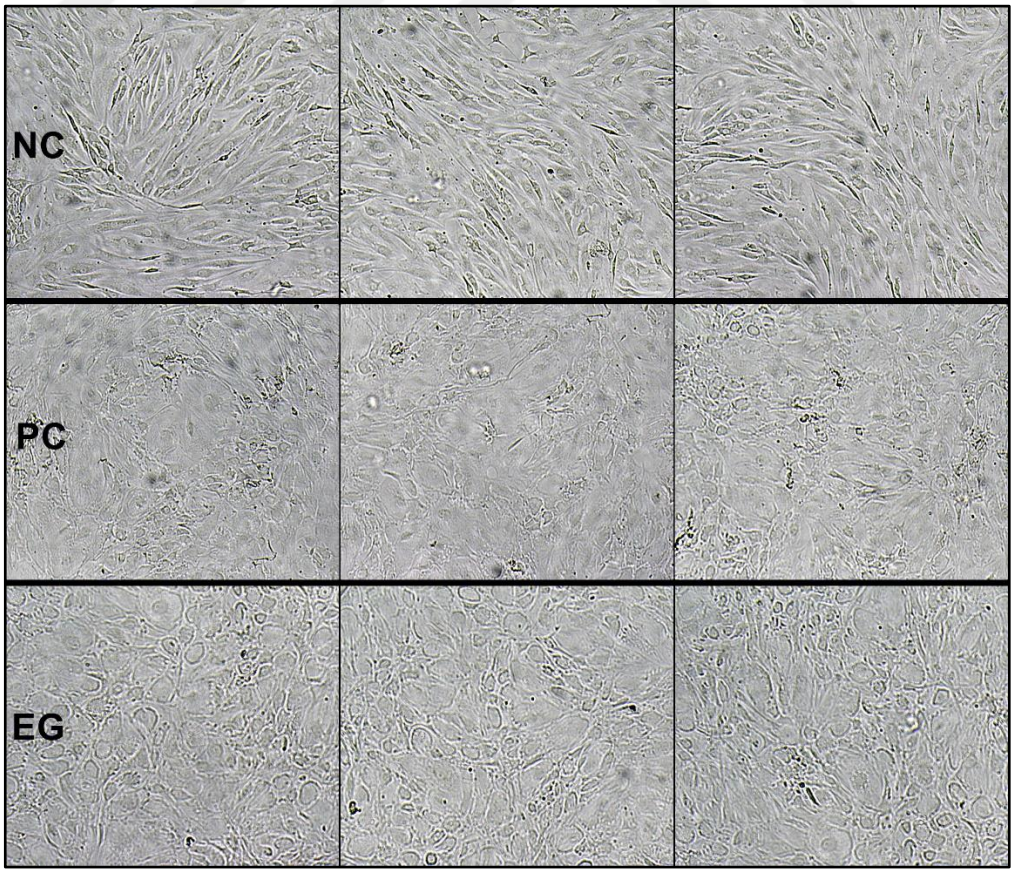

Figure 3.16. Morphological changes upon osteogenic differentiation on the 14th day

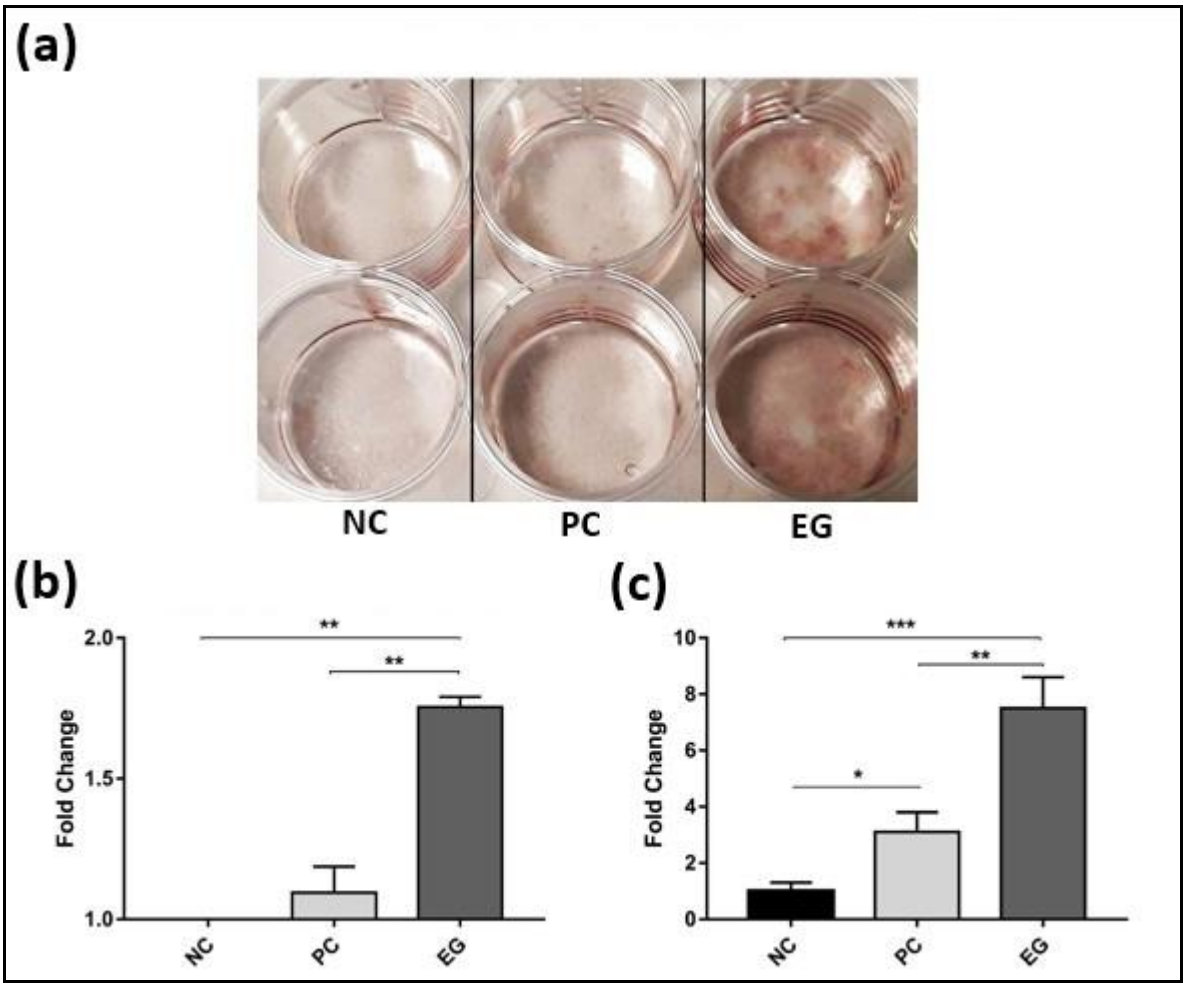

Figure 3.17. Osteogenic differentiation data. (a) Alizarin Red S staining of hNPCs upon differentiation for 14 days, (b) Quantitative analysis of Alizarin Red S staining, (c) Q-PCR analysis of the Osteopontin gene expression, * $p < 0.05$

Also, a significant increase was observed in the expression of the osteopontin gene. The experimental group was 2 fold higher than the positive control whereas 4 fold higher than the negative controls.

3.7. SCRATCH ASSAY

Scratch assay allowed us to detect the effect of CCM on wound healing. The analysis showed that there were no significant differences in the 6^{th} hour among the groups. However, in the

12th hour, the wound closure in the control group; HaCat cells was 54 percent whereas, the CCM treated HaCat, namely experimental group reached 84 percent.

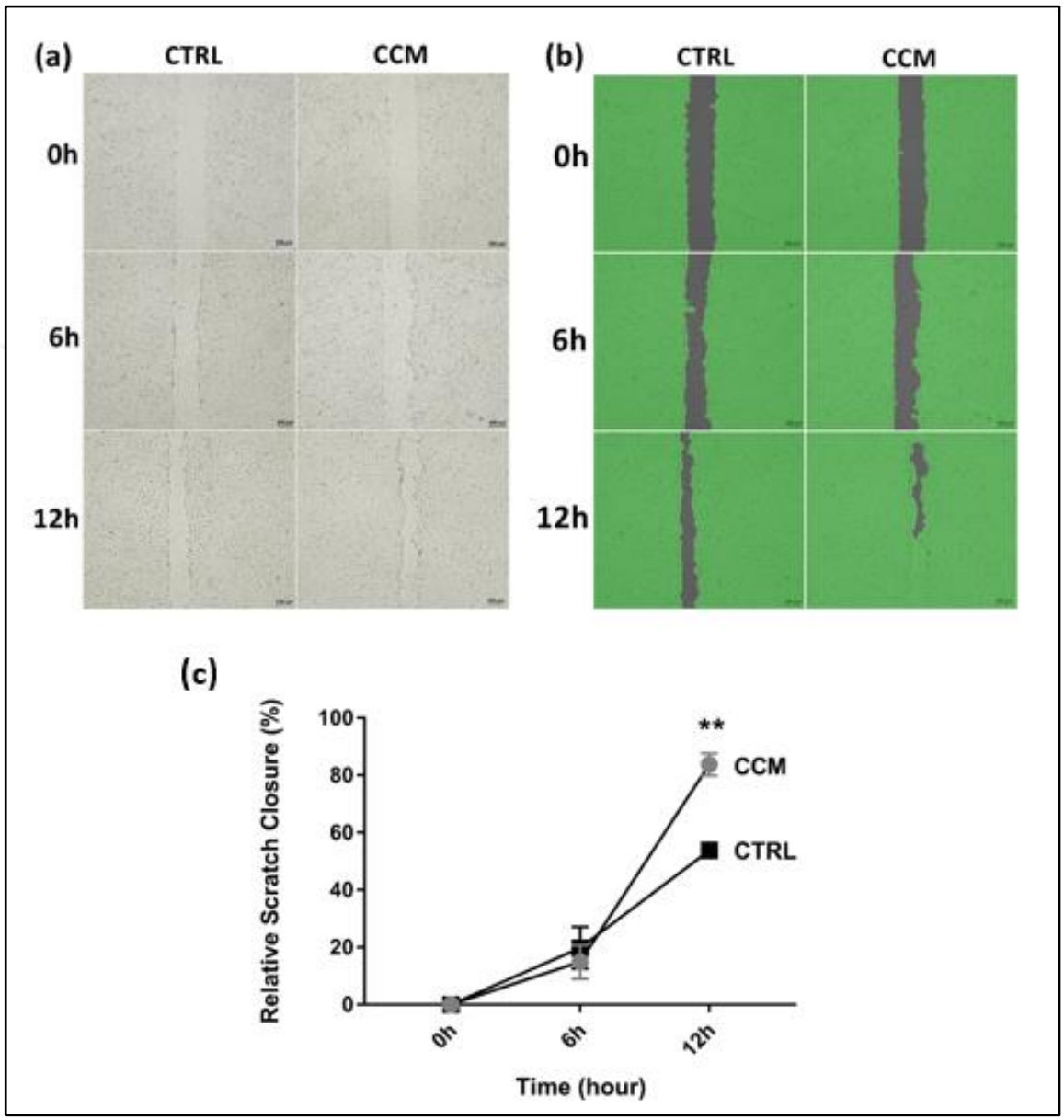

Figure 3.18. Images of scratch closure situation at different time points (0, 6, and 12 hours). (a) The cells under the microscope, (b) Wimasis analysis view. Scale Bar: 200 µm, (c) Analysis of scratch closure, * $p < 0.05$

3.8. TUBE FORMATION ASSAY

The effect of CCM and hCCs on angiogenesis was investigated. It was shown that there was a significant difference that was approximately 2 fold changes in the number of branches among control group (HUVECS) versus CCM treated HUVECS and directly hCCs.

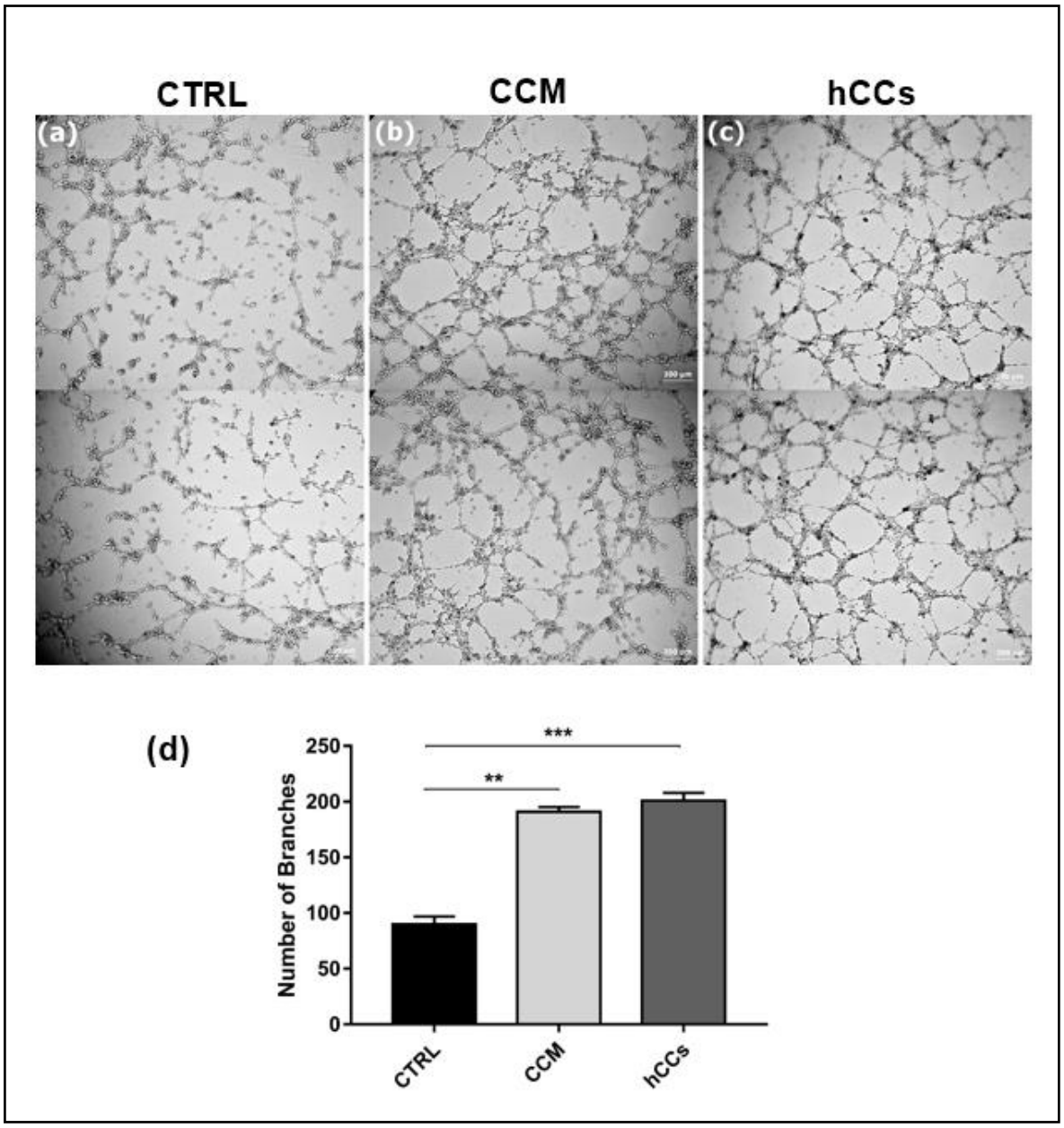

Figure 3.19. Tube formation data. Microscopic images belonged to (a) Control, HUVECs, (b) CCM treated HUVECs, (c) hCCs, Scale bar: 200 μm, (d) Analysis of Tube Formation with Wimasis, * $p < 0.05$

4. DISCUSSION

The cumulus cells are so valuable that they directly affect oocyte nuclear maturation, fertilization, and embryological development [83]. It was stated in different studies that the removal of the cumulus cells caused undesirable in vitro maturation (IVM) results in various species such as pigs, murine, bovine, and porcine. Even, in humans, the enhancing of IVM outcomes by the use of CCM was reported [84]. Nevertheless, in the ICSI process, a step of the whole IVF, describing the injection of a sperm into oocyte' cytoplasm by fine glass needle, "partial" removing or stripping of CCs are required to evaluate or grade egg maturity, to better view and pinpoint manipulation to oocyte and so unintended injection of CC' DNA into the egg was prevented thanks to removing treatment [85]. In this study, partially removed tissues were used to isolate CCs. The expression of specific genes belonging to the CCs was verified in isolated cells, and the morphology of them was confirmed with photographs from previous studies on this subject.

The specific biological event in CCs is cumulus expansion, namely the formation of HA-rich ECM structure. The presence of genes involved in cumulus expansion and matrix assembly which are HAS2, PTX3, and COX2 [86] was proved by conventional PCR and visualized by gel electrophoresis. Moreover, CX43 was also evaluated for characterization because it is responsible for creating CCs-specific gap junctions allowing material transferring between the oocyte and CCs [12]. In parallel with the existing information, the expression of CCs-specific genes in the cells ratified the homogeneity of the population in the isolated cells.

Exclusive of investigating CCs-specific gene expressions, it was targeted to compare the morphology of isolated hCCs with existing ones. Predominantly, images of the CCs shared by other researchers are photographs taken in IVF laboratories. These images contain the egg and the surrounding cumulus cells before in vitro fertilization given in figure 1. Accessible views were consistent with the image of interested tissue in this work. The acquired tissues were the same in terms of morphology. However, very few of the studies so far include microscopic images of cumulus cells in cell culture [87] [88]. The portion of these pertain to bovine, not human, and morphology of them belonging to human have not examined in detail [89]. When evaluated in this context, microscopic images of human CCs are quite special and precious and have been introduced to the world of science exclusively.

When the morphology of the hCCs was monitored under the microscope, the cells had a completely different morphology by the end of the week upon seeding. The cells' initially star-like appearance later became spindle-like, however, they acquired a senescence appearance as the time passed. This situation can be explained by two reasons. First, in mammalian females, ovulation, which is the releasing of mature egg from the ovary, occurs on the 14^{th} day of their menstrual cycle. During ovulation, CCs also remain around the egg [90]. In the event of fertilization, the fertilized egg implants to the wall of the uterus and the embryo develops, however unfertilized egg withers away and the menstrual cycle occurs. Second, findings indicate that hCCs have a mechanism to undergo apoptosis [91]. Some parameters can change their apoptotic markers profile such as females' age or exposure of CCs to sperm. In the human body, oocyte prevents CCs apoptosis by oocyte-secreted factors and particularly BMP15 and BMP6 which act anti-apoptotic characteristics [92]. In this study, the culturing model for the cumulus cells in which there is no contact with the egg cells might be one of the reasons for their apoptosis. Besides, considering the duration of the menstrual cycle, it is expected for the cells to take on a senescence appearance in a short time.

Additionally, the presence of angiogenic markers in hCCs was also detected. Angiogenesis is related to follicular growth in the ovarian cortex and is regulated separately in each follicle. Stromal blood vessels play a crucial role during nutrients and oxygen transferring to primordial and primary follicles by passive diffusion [93]. VEGF and their receptors are the main regulators of angiogenesis. They are synthesized by human theca, granulosa cells, and rat cumulus cells. Also, the localization of VEGF at granulosa and cumulus cells has been shown with immunofluorescence-based assay [94]. The synthesis of VEGF by GCs and theca cells provides the formation of a strong vascular network. The growth and production of micro-vessels are extremely fast in female's reproductive tissues. Among them, the highest blood flow rates per unit of tissue pertain to corpus luteum, which is the remained structure upon the ovulation of eggs and the main reservoir of circulating progesterone hormone. Upon its construction, it is vascularized by GCs very quickly [95]. Considering that the origin of CCs is early GCs, their angiogenesis potential is very high. This was proven in the isolated CCs by the gene expression analysis of angiogenic markers. In the majority of researches, endothelial cells such as HUVECs are used as an *in vitro* angiogenesis model [96]. Our study suggests that CC may be an alternative angiogenesis model to test several

parameters including factors affecting new blood vessel formation. This was also supported by the gene expression analysis in which VWF along with VEGF and its receptors, were found positive in hCCs. VWF is a blood glycoprotein that takes a role in hemostasis [97]. Since hemostasis and angiogenesis are also steps in a wound healing process, CCs might play a role in it. The result of scratch and tube formation assays were evidential for this argument.

What makes so special of CCs is the enriched hyaluronic acid found in their extracellular matrix. The formation of this matrix leads to a significant increase in the volume of COC, a process called cumulus expansion. This phenomenon is essential for meiotic maturation and gaining the developmental competence of the egg [98]. The most abundant component of this ECM is hyaluronic acid synthesized by HAS2 in CCs. The accumulation and assembly of HA between the CCs produce a spongy and an elastic structure that can promote the extrusion of the oocyte during ovulation. Also, for successful fertilization, the special matrix of COCs acts as a selective barrier that does not allow penetration of enzymatically or functionally incomplete sperms [99]. Salustri and his colleagues have examined the amount of synthesized HA in COCs during the pre-ovulatory phase and ovulatory phase. They showed that the overall HA amount and cell number *in vivo* ovulated COC were approximately three times greater than *in vitro* expanded COC [100]. Further investigations suggest that amount of synthesized HA by CCs depends on various parameters including the presence of FSH and EGF as being the main promoters of the synthesis. Also, prostaglandin, a group of lipids, affects cumulus expansion and HA accumulation [101]. Considering that the synthesis of hyaluronic acid is affected by the considerable amount of factors naturally provided by the human body, the amount of HA obtained in this study should not be underestimated.

Even the smallest amount of hyaluronic acid is very valuable because it is a naturally derived GAG with a wide range of usage areas [102]. On the other hand, the optimization of *in vitro* HA production is very tedious and expensive [103]. The yield of bacterial fermentation is characteristically low (0.1g/g glucose) in addition to its hardship to obtain HW-HA economically from bovine vitreous humour and rooster combs [104]. Thus, obtaining HA from discarded cumulus tissue is influential. Moreover, many *in vivo* studies and *in vitro* experiments have demonstrated that HA fragments promoted angiogenesis and wound healing. Scientists explain the underlying mechanisms as the interaction between CD44 and

HA oligosaccharides showing a pro-mitotic effect that stimulate MMP2 and MMP9 production. Through this way, cell invasion via ECM increases to help vessel sprouting [105]. As a result, maximum efficiency is obtained from tube formation and scratch assays suggesting CCs as an alternative model for angiogenesis that maybe caused by the angiogenic properties of hyaluronic acid.

Various studies depict that hyaluronic acid improves not only the wound healing and angiogenesis but also cell differentiation [106-108]. For instance, Takahashi and his colleagues reported that HA was able to induce osteoblastic differentiation of newborn rat calvaria cells [109]. Besides, it was proven in many studies that HA facilitated chondrogenesis [110, 111]. In the light of this information, nucleus pulposus cells that lost their cartilaginous properties were repaired with cumulus cell-derived hyaluronic acid-containing differentiation media. The results were satisfactory. The nucleus pulposus tissue involves notochordal remnants which enable differentiation [112]. To determine the differentiation capacity of hNPCs, stem cell surface markers were analyzed to show mesechymal stem cells properties which were compatible with previous studies [113, 114].

Moreover, hNPCs are highly successful in encountering the minimum requirements specified by ISCT to qualify the cells as a mesenchymal cell [115]. NPCs displayed adherent properties along with the presence of CD73, CD90, and CD105 and lack of hematopoietic markers including CD34, CD45, CD14. Among the positive surface proteins, CD105 showed reduced expression as opposed to the others. CD105 is generally up-regulated in proliferating endothelial cells and has a role in angiogenesis [116]. At this point, CD105 expression can be expected to be low in the nucleus pulposus cells and reflect the avascular characteristic of the IVD [117].

Also, the potential of differentiation to other lineages of hNPCs was evaluated in our study. CCM containing differentiation agents stimulated hNPCs for better osteogenesis. Differentiation of hNPCs to osteocytes and enhancing its chondrogenecity demonstrated that hNPCs had stem cell characteristics. The duration time for the differentiation assays lasts at least ten days [118] so the maintenance of cells' stability is a very important to concern about. Considering our MTS assay-based growth data of hNPCs and previous studies involving stem cells [119], one can conclude that NPCs have a longer cell-doubling time than various stem cells. These aspects of NPCs may make them more preferable in IVD-related studies.

Finally, our study depicts that the conditioned medium harvested from the cumulus cells are enriched in hyaluronic acid. It enhanced the chondrogenic potential of nucleus pulposus cells and may be used as an alternative cell-related therapy to treat chondral-degenerative diseases.

5. CONCLUSION

Within the scope of this study, the capacity of human cumulus cells in the treatment of chondro-degenerated nucleus pulposus cells was thoroughly investigated. According to our results, the high hyaluronic acid content of cumulus cells was discovered using human primary culture samples derived from patients. Interestingly, we discovered a potent differentiation-inducing effect of hyaluronic acid on nucleus pulposus cells that indicated stemness characteristics. Furthermore, -not only- chondroid property of human nucleus pulposus cells was stimulated when they were cultured in a conditioned medium of human cumulus cells but also their ability to differentiate into osteocytes was enhanced. Most strikingly, remarkable pro-angiogenic and wound healing effects of hyaluronic acid-rich human cumulus cells were uncovered both in tube formation and scratch assays, where a significant increase in the number of branches and wound closure area, respectively, was detected only in groups cultured in cumulus cell-conditioned medium compared to the control. Finally, the observation where cumulus cells were able to form the endothelial cell-like branches on matrigel underscores these cells as a valuable and novel model in addition to the widely used angiogenesis model of HUVEC cells.

REFERENCES

1. Dumesic DA, Meldrum DR, Katz-Jaffe MG, Krisher RL, Schoolcraft WB. Oocyte environment: follicular fluid and cumulus cells are critical for oocyte health. *Fertility and Sterility*. 2015;103(2):303-16.

2. Rienzi L, Balaban B, Ebner T, Mandelbaum J. The oocyte. *Human Reproduction*. 2012;27:21-2.

3. Elder K, Dale B. Oocyte retrieval and embryo culture. *In-vitro fertilization*. 2010:157-90.

4. Robker RL, Hennebold JD, Russell DL. Coordination of ovulation and oocyte maturation: a good egg at the right time. *Endocrinology*. 2018;159(9):3209-18.

5. Ebner T, Moser M, Sommergruber M, Shebl O, Tews G. Incomplete denudation of oocytes prior to ICSI enhances embryo quality and blastocyst development. *Human Reproduction*. 2006;21(11):2972-7.

6. Malter HE, Cohen J. Partial zona dissection of the human oocyte: a nontraumatic method using micromanipulation to assist zona pellucida penetration. *Fertility and Sterility*. 1989;51(1):139-48.

7. Huang Z, Wells D. The human oocyte and cumulus cells relationship: new insights from the cumulus cell transcriptome. *Molecular Human Reproduction*. 2010;16(10):715-25.

8. Alam MH, Miyano T. Interaction between growing oocytes and granulosa cells in vitro. *Reproductive Medicine and Biology*. 2020;19(1):13-23.

9. Green LJ, Shikanov A. In vitro culture methods of preantral follicles. *Theriogenology*. 2016;86(1):229-38.

10. Sanfins A, Rodrigues P, Albertini DF. GDF-9 and BMP-15 direct the follicle symphony. *Journal of Assisted Reproduction and Genetics*. 2018;35(10):1741-50.

11. Jeppesen J, Kristensen S, Nielsen M, Humaidan P, Dal Canto M, Fadini R, et al. LH-receptor gene expression in human granulosa and cumulus cells from antral and

preovulatory follicles. *The Journal of Clinical Endocrinology and Metabolism*. 2012;97:1524-31.

12. Wang HX, Tong D, El-Gehani F, Tekpetey FR, Kidder GM. Connexin expression and gap junctional coupling in human cumulus cells: contribution to embryo quality. *Journal of Cellular and Molecular Medicine*. 2009;13(5):972-84.

13. Russell DL, Robker RL. Cumulus Cells. *Encyclopedia of reproduction.* 2018:43-6.

14. Cillo F, Brevini T, Antonini S, Paffoni A, Ragni G, Gandolfi F. Association between human oocyte developmental competence and expression levels of some cumulus genes. *Reproduction*. 2007;134:645-50.

15. Clarke HJ. History, origin, and function of transzonal projections: the bridges of communication between the oocyte and its environment. *Animal Reproduction (AR)*. 2018;15(3):215-23.

16. Xu B, Noohi S, Shin JS, Tan SL, Taketo T. Bi-directional communication with the cumulus cells is involved in the deficiency of XY oocytes in the components essential for proper second meiotic spindle assembly. *Developmental Biology*. 2014;385(2):242-52.

17. Mira A. Why is meiosis arrested? *Journal of Theoretical Biology*. 1998;194(2):275-87.

18. Pan B, Li J. The art of oocyte meiotic arrest regulation. *Reproductive Biology and Endocrinology: RB&E*. 2019;17(1):8-1.

19. Brown HM, Dunning KR, Robker RL, Boerboom D, Pritchard M, Lane M, et al. ADAMTS1 Cleavage of versican mediates essential structural remodeling of the ovarian follicle and cumulus-oocyte matrix during ovulation in mice1. *Biology of Reproduction*. 2010;83(4):549-57.

20. Oren-Benaroya R, Orvieto R, Gakamsky A, Pinchasov M, Eisenbach M. The sperm chemoattractant secreted from human cumulus cells is progesterone. *Human Reproduction*. 2008;23(10):2339-45.

21. Lin Y, Mahan K, Lathrop W, Myles D, Primakoff P. A hyaluronidase activity of the sperm plasma membrane protein PH-20 enables sperm to penetrate the cumulus cell layer surrounding the egg. *The Journal of Cell Biology*. 1994;125:1157-63.

22. Shimada M, Yanai Y, Okazaki T, Noma N, Kawashima I, Mori T, et al. Hyaluronan fragments generated by sperm-secreted hyaluronidase stimulate cytokine/chemokine production via the TLR2 and TLR4 pathway in cumulus cells of ovulated COCs, which may enhance fertilization. *Development*. 2008;135(11):2001-11.

23. Goud AP, Goud PT, Diamond MP, Gonik B, Abu-Soud HM. Reactive oxygen species and oocyte aging: role of superoxide, hydrogen peroxide, and hypochlorous acid. *Free Radical Biology & Medicine*. 2008;44(7):1295-304.

24. Necas J, Bartosikova L, Brauner P, Kolář J. Hyaluronic acid (Hyaluronan): A review. *Veterinarni Medicina*. 2008;53(8):397-411.

25. Selyanin M, Boykov P, Khabarov V, Polyak F. The history of hyaluronic acid discovery. *Foundational research and initial use*. 2015:1-8.

26. Necas J, Bartosikova L, Brauner P, Kolar J. Hyaluronic acid (hyaluronan): A review. *Veterinarni Medicina*. 2008;53(8):397-411.

27. Menaa F. Hyaluronic acid and derivatives for tissue engineering. *Journal of Biotechnology & Biomaterials*. 2011;3:001.

28. de Oliveira JD, Carvalho LS, Gomes AMV, Queiroz LR, Magalhães BS, Parachin NS. Genetic basis for hyper production of hyaluronic acid in natural and engineered microorganisms. *Microbial Cell Factories*. 2016;15(1):119.

29. Cowman M, Schmidt T, Raghavan P, Stecco A. Viscoelastic properties of hyaluronan in physiological conditions. *F1000Research*. 2015;4:622.

30. Casale J, Crane JS. *Biochemistry, glycosaminoglycans*. Florida: StatPearls Press; 2020.

31. Itano N, Chanmee T, Kimata K. Hyaluronan synthase 1-3 (HAS1-3). *Handbook of glycosyltransferases and related genes*. 2014:865-72.

32. Weigel PH. Functional characteristics and catalytic mechanisms of the bacterial hyaluronan synthases. *IUBMB Life*. 2002;54(4):201-11.

33. Chistyakov DV, Astakhova AA, Azbukina NV, Goriainov SV, Chistyakov VV, Sergeeva MG. High and low molecular weight hyaluronic acid differentially influences oxylipins synthesis in course of neuroinflammation. *International Journal of Molecular Sciences*. 2019;20(16):3894.

34. Li J, Qiao M, Ji Y, Lin L, Zhang X, Linhardt RJ. Chemical, enzymatic and biological synthesis of hyaluronic acids. *International Journal of Biological Macromolecules*. 2020;152:199-206

35. Sze J, Brownlie J, Love C. Biotechnological production of hyaluronic acid: a mini-review. *3 Biotech*. 2016;6(1):67

36. Kogan G, Šoltés L, Stern R, Schiller J, Mendichi R. Hyaluronic acid: its function and degradation in vivo systems. *Studies in Natural Products Chemistry*. 2008;34:789-882.

37. Soltés L, Mendichi R, Kogan G, Schiller J, Stankovska M, Arnhold J. Degradative action of reactive oxygen species on hyaluronan. *Biomacromolecules*. 2006;7:659-68.

38. Gura E, Hückel M, Müller P. Specific degradation of rheological hyaluronic acid and its properties. *Polymer Degradation and Stability*. 1998;59:297-302.

39. Stern R, Jedrzejas MJ. Hyaluronidases: their genomics, structures, and mechanisms of action. *Chemical Reviews*. 2006;106(3):818-39.

40. Li C, Wang L-X. Endoglycosidases for the synthesis of polysaccharides and glycoconjugates. *Advances in Carbohydrate Chemistry and Biochemistry*. 2016;73:73-116.

41. Peng C, Wang Q, Wang S, Wang W, Jiao R, Han W, et al. A chondroitin sulfate and hyaluronic acid lyase with poor activity to glucuronyl 4,6-O-disulfated N-acetylgalactosamine (E-type)-containing structures. *The Journal of Biological Chemistry*. 2018;293(12):4230-43.

42. Fakhari A, Berkland C. Applications and emerging trends of hyaluronic acid in tissue engineering, as a dermal filler and in osteoarthritis treatment. *Acta Biomaterialia*. 2013;9(7):7081-92.

43. Saranraj P, Naidu M. Hyaluronic acid production and its applications a review. *Int J Pharm Biol Arch*. 2013;4(5):853-59.

44. Lm N, Balakrishnan R, Sivaprakasam S. Optimization and effect of dairy industrial waste as media components in the production of hyaluronic acid by Streptococcus thermophilus. *Preparative Biochemistry & Biotechnology*. 2016;46(6):628-638.

45. Gonzalez ACdO, Costa TF, Andrade ZdA, Medrado ARAP. Wound healing - a literature review. *Anais Brasileiros de Dermatologia*. 2016;91(5):614-20.

46. Frenkel JS. The role of hyaluronan in wound healing. *International Wound Journal*. 2014;11(2):159-63.

47. Martin J, Midgley A, Meran S, Woods E, Bowen T, Phillips AO, et al. Tumor necrosis factor-stimulated gene 6 (TSG-6)-mediated interactions with the inter-α-inhibitor heavy chain 5 facilitate tumor growth factor β1 (TGFβ1)-dependent fibroblast to myofibroblast differentiation. *The Journal of Biological Chemistry*. 2016;291(26):13789-801.

48. Halloran C, Slavin J. Pathophysiology of wound healing. *Surgery*. 2002;20(5):5-1.

49. Misra S, Hascall VC, Markwald RR, Ghatak S. Interactions between hyaluronan and its receptors (CD44, RHAMM) regulate the activities of inflammation and cancer. *Frontiers in Immunology*. 2015;6:201-1.

50. Lawson C, Wolf S. ICAM-1 signaling in endothelial cells. *Pharmacological Reports: PR*. 2009;61:22-32.

51. Wang Y, Cao M, Liu Y, He Y, Yang C, Gao F. CD44 mediates oligosaccharides of hyaluronan-induced proliferation, tube formation and signal transduction in endothelial cells. *Experimental Biology and Medicine*. 2011;236:84-90.

52. Osseiran S, Cruz JD, Jeong S, Wang H, Fthenakis C, Evans CL. Characterizing stratum corneum structure, barrier function, and chemical content of human skin with coherent Raman scattering imaging. *Biomedical Optics Express*. 2018;9(12):6425-43.

53. Aydemir I, Öztürk Ş, Sönmez PK, Tuğlu Mİ. Mesenchymal stem cells in skin wound healing. *Anatomy: International Journal of Experimental & Clinical Anatomy*. 2016;10(3).

54. Chitturi RT, Balasubramaniam AM, Parameswar RA, Kesavan G, Haris KTM, Mohideen K. The role of myofibroblasts in wound healing, contraction and its clinical implications in cleft palate repair. *Journal of International Oral Health: JIOH*. 2015;7(3):75-80.

55. Mahla RS. Stem cells applications in regenerative medicine and disease therapeutics. *International Journal of Cell Biology*. 2016;2016:6940283.

56. Solis MA, Chen Y-H, Wong TY, Bittencourt VZ, Lin Y-C, Huang LLH. Hyaluronan regulates cell behavior: a potential niche matrix for stem cells. *Biochemistry Research International*. 2012;346972.

57. Han Y, Li X, Zhang Y, Han Y, Chang F, Ding J. Mesenchymal stem cells for regenerative medicine. *Cells*. 2019;8(8):886.

58. Dominici M, Le Blanc K, Mueller I, Slaper-Cortenbach I, Marini F, Krause D, et al. Minimal criteria for defining multipotent mesenchymal stromal cells. The international society for cellular therapy position statement. *Cytotherapy*. 2006;8(4):315-7.

59. Clause KC, Liu LJ, Tobita K. Directed stem cell differentiation: the role of physical forces. *Cell Communication & Adhesion*. 2010;17(2):48-54.

60. Solis MA, Chen Y-H, Wong TY, Bittencourt VZ, Lin Y-C, Huang LL. Hyaluronan regulates cell behavior: a potential niche matrix for stem cells. *Biochemistry Research International*. 2012;2012:346972.

61. Roughley PJ, Lamplugh L, Lee ER, Matsumoto K, Yamaguchi Y. The role of hyaluronan produced by Has2 gene expression in development of the spine. *Spine*. 2011;36(14):914-20.

62. Gerecht S, Burdick JA, Ferreira LS, Townsend SA, Langer R, Vunjak-Novakovic G. Hyaluronic acid hydrogel for controlled self-renewal and differentiation of human embryonic stem cells. *Proceedings of the National Academy of Sciences*. 2007;104(27):11298-303.

63. Feng X, Zhang J, Smuga-Otto K, Tian S, Yu J, Stewart R, et al. Protein kinase C mediated extraembryonic endoderm differentiation of human embryonic stem cells. *Stem Cells (Dayton, Ohio)*. 2012;30(3):461-70.

64. Llames S, García-Pérez E, Meana Á, Larcher F, del Río M. Feeder layer cell actions and applications. *Tissue Engineering Part B, Reviews*. 2015;21(4):345-53.

65. Kayalioglu G. The vertebral column and spinal meninges. *The Spinal Cord*. 2009:17-36.

66. Tamang BK. The role of cell clusters in intervertebral disc degeneration and its relevance behind repair. *Archivos de Medicina*. 2017;3(3):15.

67. Nedresky D, Singh G. *Anatomy, back, nucleus pulposus*. Florida: StatPearls Press; 2020.

68. Marcolongo M, Sarkar S, Ganesh N. 7.11 Trends in materials for spine surgery. *Comprehensive biomaterials II*. 2017:175-98.

69. Risbud MV, Shapiro IM. Notochordal cells in the adult intervertebral disc: new perspective on an old question. *Critical Reviews in Eukaryotic Gene Expression*. 2011;21(1):29-41.

70. Yoon ST, Patel NM. Molecular therapy of the intervertebral disc. *European Spine Journal: Official Publication of the European Spine Society, the European Spinal Deformity Society, and the European Section of the Cervical Spine Research Society*. 2006;15:379-88.

71. Power K, Grad S, Rutges J, Creemers L, Rijen M, O'Gaora P, et al. Identification of cell surface-specific markers to target human nucleus pulposus cells: Expression of carbonic anhydrase XII varies with age and degeneration. *Arthritis and Rheumatism*. 2011;63:3876-86.

72. Choi H, Johnson ZI, Risbud MV. Understanding nucleus pulposus cell phenotype: a prerequisite for stem cell based therapies to treat intervertebral disc degeneration. *Current Stem Cell Research & Therapy*. 2015;10(4):307-16.

73. Stosiek P, Kasper M, Karsten U. Expression of cytokeratin and vimentin in nucleus pulposus cells. *Differentiation*. 1988;39(1):78-81.

74. Newell N, Little JP, Christou A, Adams MA, Adam CJ, Masouros SD. Biomechanics of the human intervertebral disc: A review of testing techniques and results. *Journal of the Mechanical Behavior of Biomedical Materials*. 2017;69:420-34.

75. Ma D, Liang Y, Wang D, Liu Z, Zhang W, Ma T, et al. Trend of the incidence of lumbar disc herniation: decreasing with aging in the elderly. *Clinical Interventions in Aging*. 2013;8:1047-50.

76. Konieczny MR, Reinhardt J, Prost M, Schleich C, Krauspe R. Signal intensity of lumbar disc herniations: correlation with age of herniation for extrusion, protrusion, and sequestration. *International Journal of Spine Surgery*. 2020;14(1):102-7.

77. Miller J, Cho J, Michael M, Saouaf R, Towfigh S. Role of imaging in the diagnosis of occult hernias. *JAMA Surgery*. 2014;149(10):1077-1080.

78. Mern DS, Beierfuß A, Thomé C, Hegewald AA. Enhancing human nucleus pulposus cells for biological treatment approaches of degenerative intervertebral disc diseases: a systematic review. *Journal of Tissue Engineering and Regenerative Medicine*. 2014;8(12):925-36.

79. Calikoglu Koyuncu AC, Gurel Pekozer G, Ramazanoglu M, Torun Kose G, Hasirci V. Cartilage tissue engineering on macroporous scaffolds using human tooth germ stem cells. *Journal of Tissue Engineering and Regenerative Medicine*. 2017;11(3):765-77.

80. Gürel Peközer G, Kose G, Hasirci V. Influence of co-culture on osteogenesis and angiogenesis of bone marrow mesenchymal stem cells and aortic endothelial cells. *Microvascular Research*. 2016;108:1-9.

81. Liang C-C, Park AY, Guan J-L. In vitro scratch assay: a convenient and inexpensive method for analysis of cell migration in vitro. *Nature Protocols*. 2007;2(2):329.

82. Zhou Q, Kiosses WB, Liu J, Schimmel P. Tumor endothelial cell tube formation model for determining anti-angiogenic activity of a tRNA synthetase cytokine. *Methods (San Diego, Calif)*. 2008;44(2):190-5.

83. Sadat Tahajjodi S, Farashahi Yazd E, Agha-Rahimi A, Aflatoonian R, Ali Khalili M, Mohammadi M, et al. Biological and physiological characteristics of human cumulus cells in adherent culture condition. *International Journal of Reproductive Biomedicine*. 2020;18(1):1-10.

84. Wongsrikeao P, Kaneshige Y, Ooki R, Taniguchi M, Agung B, Nii M, et al. Effect of the removal of cumulus cells on the nuclear maturation, fertilization and development of porcine oocytes. *Reproduction in Domestic Animals*. 2005;40(2):166-70.

85. Evison M, Pretty C, Taylor E, Franklin C. Human recombinant hyaluronidase (Cumulase®) improves intracytoplasmic sperm injection survival and fertilization rates. *Reproductive Biomedicine Online*. 2009;18(6):811-4.

86. Du M, Fu X, Zhou Y, Zhu S. Effects of trichostatin A on cumulus expansion during mouse oocyte maturation. *Asian-Australasian Journal of Animal Sciences*. 2013;26(11):1545.

87. Tahajjodi S, Farashahi Yazd E, Agha-Rahimi A, Aflatoonian R, Khalili ma, Mohammadi M, et al. Biological and physiological characteristics of human cumulus cell in adherent culture condition. *International Journal of Reproductive BioMedicine (IJRM)*. 2020;18:1-10.

88. Chermuła B, Kranc W, Jopek K, Budna-Tukan J, Hutchings G, Dompe C, et al. Human cumulus cells in long-term in vitro culture reflect differential expression profile of genes responsible for planned cell death and aging—a study of new molecular markers. *Cells*. 2020;9(5):1265.

89. Gajda B, Katska-Ksiazkiewicz L, Ryńska B, Bochenek M, Smorag Z. Survival of bovine fibroblasts and cumulus cells after vitrification. *Cryo Letters*. 2007;28:271-9.

90. Carrell D, Middleton R, Peterson C, Jones K, Urry R. Role of the cumulus in the selection of morphologically normal sperm and induction of the acrosome reaction during human in vitro fertilization. *Archives of Andrology*. 1993;31(2):133-7.

91. Moffatt O, Drury S, Tomlinson M, Afnan M, Sakkas D. The apoptotic profile of human cumulus cells changes with patient age and after exposure to sperm but not in relation to oocyte maturity. *Fertility and Sterility*. 2002;77(5):1006-11.

92. Hussein TS, Froiland DA, Amato F, Thompson JG, Gilchrist RB. Oocytes prevent cumulus cell apoptosis by maintaining a morphogenic paracrine gradient of bone morphogenetic proteins. *Journal of Cell Science*. 2005;118(22):5257-68.

93. Da Broi MG, Giorgi VSI, Wang F, Keefe DL, Albertini D, Navarro PA. Influence of follicular fluid and cumulus cells on oocyte quality: clinical implications. *Journal of Assisted Reproduction and Genetics*. 2018;35(5):735-51.

94. Abbas MM, Evans JJ, Sin IL, Gooneratne A, Hill A, Benny PS. Vascular endothelial growth factor and leptin: regulation in human cumulus cells and in follicles. *Acta Obstetricia et Gynecologica Scandinavica*. 2003;82(11):997-1003.

95. Chermuła B, Brązert M, Iżycki D, Ciesiółka S, Kranc W, Celichowski P, et al. New gene markers of angiogenesis and blood vessels development in porcine ovarian granulosa cells during short-term primary culture in vitro. *BioMed Research International*. 2019;2019:6545210.

96. Yukawa H, Suzuki K, Aoki K, Arimoto T, Yasui T, Kaji N, et al. Imaging of angiogenesis of human umbilical vein endothelial cells by uptake of exosomes secreted from hepatocellular carcinoma cells. *Scientific Reports*. 2018;8(1):1-12.

97. Cumming A, Grundy P, Keeney S, Lester W, Enayat S, Guilliatt A, et al. An investigation of the von Willebrand factor genotype in UK patients diagnosed to have type 1 von Willebrand disease. *Thrombosis and Haemostasis*. 2006;96(11):630-41.

98. Nevoral J, Orsák M, Klein P, Petr J, Dvořáková M, Weingartová I, et al. Cumulus cell expansion, its role in oocyte biology and perspectives of measurement: a review. *Scientia Agriculturae Bohemica*. 2014;45:212-25.

99. Salustri A, Fulop C. Role of hyaluronan during ovulation and fertilization. *Hyaluronan Today*. 1998;2(2).

100. Salustri A, Yanagishita M, Underhill CB, Laurent TC, Hascall VC. Localization and synthesis of hyaluronic acid in the cumulus cells and mural granulosa cells of the preovulatory follicle. *Developmental Biology*. 1992;151(2):541-51.

101. Goverde HJM. The enhancement by prostaglandin E2 of cumulus cell outgrowth in vitro. *Prostaglandins*. 1993;45(3):241-7.

102. Dhanusha B. Hyaluronic acid and its applications. *Journal of Medical and Health Sciences*. 2015;4(2).

103. Boeriu CG, Springer J, Kooy FK, van den Broek LAM, Eggink G. Production methods for hyaluronan. *International Journal of Carbohydrate Chemistry*. 2013;2013:624967.

104. Saranraj P, Naidu MA. Hyaluronic acid production and its applications-a review. *International Journal of Pharmaceutical and Biological Archive*. 2013;4:853-9.

105. Pardue EL, Ibrahim S, Ramamurthi A. Role of hyaluronan in angiogenesis and its utility to angiogenic tissue engineering. *Organogenesis*. 2008;4(4):203-14.

106. Cañibano-Hernández A, Saenz del Burgo L, Espona-Noguera A, Orive G, Hernández RM, Ciriza Js, et al. Hyaluronic acid promotes differentiation of mesenchymal stem cells from different sources toward pancreatic progenitors within three-dimensional alginate matrixes. *Molecular Pharmaceutics*. 2019;16(2):834-45.

107. Simpson RM, Hong X, Wong MM, Karamariti E, Bhaloo SI, Warren D, et al. Hyaluronan is crucial for stem cell differentiation into smooth muscle lineage. *Stem Cells (Dayton, Ohio)*. 2016;34(5):1225-38.

108. Maharjan AS, Pilling D, Gomer RH. High and low molecular weight hyaluronic acid differentially regulate human fibrocyte differentiation. *PloS One*. 2011;6(10):e26078.

109. Takahashi M, Kawa-uchi T, Wakabayashi Y. Hyaluronic acid induces osteoblastic differentiation of osteoblast progenitor cells. *Orthopaedic research society*. 1999:578.

110. Jakobsen RB, Shahdadfar A, Reinholt FP, Brinchmann JE. Chondrogenesis in a hyaluronic acid scaffold: comparison between chondrocytes and MSC from bone marrow and adipose tissue. *Knee Surgery, Sports Traumatology, Arthroscopy*. 2010;18(10):1407-16.

111. Amann E, Wolff P, Breel E, van Griensven M, Balmayor ER. Hyaluronic acid facilitates chondrogenesis and matrix deposition of human adipose derived mesenchymal stem cells and human chondrocytes co-cultures. *Acta Biomaterialia*. 2017;52:130-44.

112. Gupta R. Benign Notochordal Remnant. *PET/MR imaging.* 2018:7-8.

113. Jia Z, Yang P, Wu Y, Tang Y, Zhao Y, Wu J, et al. Comparison of biological characteristics of nucleus pulposus mesenchymal stem cells derived from non-degenerative and degenerative human nucleus pulposus. *Experimental and Therapeutic Medicine*. 2017;13(6):3574-80.

114. Zhao Y, Jia Z, Huang S, Wu Y, Liu L, Lin L, et al. Age-related changes in nucleus pulposus mesenchymal stem cells: an in vitro study in rats. *Stem Cells International*. 2017;2017:6761572.

115. Lyu F-J, Cheung KM, Zheng Z, Wang H, Sakai D, Leung VY. IVD progenitor cells: a new horizon for understanding disc homeostasis and repair. *Nature Reviews Rheumatology*. 2019;15(2):102-12.

116. Nassiri F, Cusimano MD, Scheithauer BW, Rotondo F, Fazio A, Yousef GM, et al. Endoglin (CD105): a review of its role in angiogenesis and tumor diagnosis, progression and therapy. *Anticancer Research*. 2011;31(6):2283-90.

117. Duff SE, Li C, Garland JM, Kumar S. CD105 is important for angiogenesis: evidence and potential applications. *The FASEB Journal*. 2003;17(9):984-92.

118. Hurrell T, Segeritz C-P, Vallier L, Lilley KS, Cromarty AD. A proteomic time course through the differentiation of human induced pluripotent stem cells into hepatocyte-like cells. *Scientific Reports*. 2019;9(1):3270.

119. Mennan C, Brown S, McCarthy H, Mavrogonatou E, Kletsas D, Garcia J, et al. Mesenchymal stromal cells derived from whole human umbilical cord exhibit similar

properties to those derived from Wharton's jelly and bone marrow. *FEBS Open Bio*. 2016;6(11):1054-66.

APPENDIX A: FLOW CYTOMETRY OPTIMIZATION FOR HNPCS

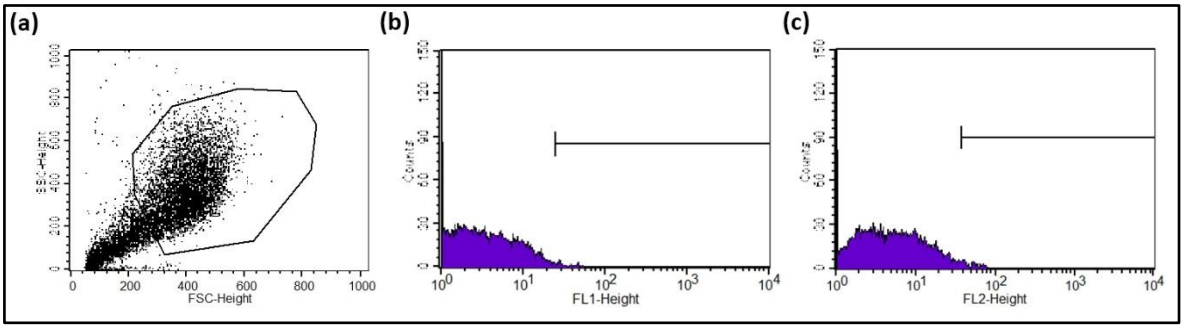

Figure A.1. Flow data of hNPCs' negative control lack of antibody treatment; (a) dot plot map, (b) FL-1 channel height and, (c) FL-2 channel height

APPENDIX B: CALIBRATION CURVE FOR HA QUANTIFICATION

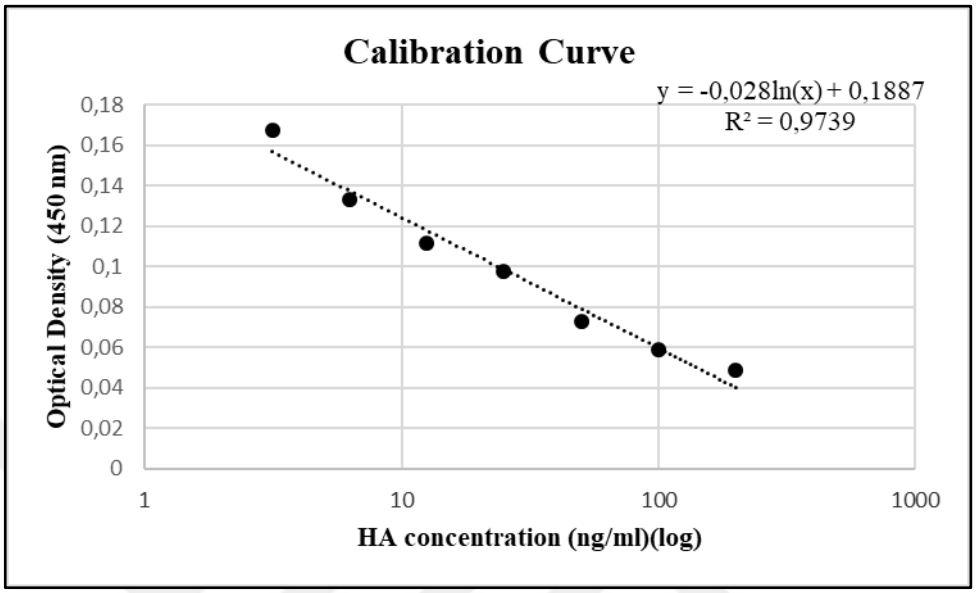

Figure B.1. Calibration curve used for calculating HA amount in the samples

APPENDIX C: ETHICAL COMMITTEE APPROVAL

T.C. YEDİTEPE ÜNİVERSİTESİ

Sayı : 37068608-6100-15- 1949 **10/09/2020**
Konu: Klinik Araştırmalar
Etik Kurul Başvurusu hk.

İlgili Makama (Esra Aydemir Çoban)

Yeditepe Üniversitesi Genetik ve Biyomühendislik Bölümü, Moleküler Biyoloji ve Diagnostik Laboratuvarı Dr./Post-doc Esra Aydemir Çoban'ın proje koordinatörü olduğu, Histoloji ve Embriyoloji AD. Dr. Öğr. Üyesi Oya Alagöz'ün sorumlu hekim olduğu **"İnsan Kumulus Hücrelerinden Türetilen Hücre Bazlı Ürünlerin Çeşitli Fizyolojik ve Terapötik Etkilerinin Araştırılması"** isimli araştırma projesine ait Klinik Araştırmalar Etik Kurulu (KAEK) Başvuru Dosyası **(1941)** kayıtlı Numaralı KAEK Başvuru Dosyası, Yeditepe Üniversitesi Klinik Araştırmalar Etik Kurulu tarafından **09.09.2020** tarihli toplantıda incelenmiştir.

Kurul tarafından yapılan inceleme sonucu, yukarıdaki isim belirtilen çalışmanın yapılmasının etik ve bilimsel açıdan uygun olduğuna karar verilmiştir. **(KAEK Karar No:1281)**

Prof. Dr. Turgay Çelik

Yeditepe Üniversitesi
Klinik Araştırmalar Etik Kurul Başkanı

Yeditepe Üniversitesi 26 Ağustos Yerleşimi, İnönü Mahallesi Kayışdağı Caddesi 34755 Ataşehir / İstanbul
T. 0216 578 00 00 www.yeditepe.edu.tr F. 0216 578 02 99